Mathematics and Computers in Simulation 241 (2026) 326–350

Contents lists available at ScienceDirect

Mathematics and Computers in Simulation

journal homepage: www.elsevier.com/locate/matcom

Original articles

Spline-based approximation for two-parameter singularly perturbed systems with large time delay with applications in science and engineering

Parvin Kumari [a], Carmelo Clavero [b,*]

[a] Manipal University Jaipur, Jaipur, India
[b] Department of Applied Mathematics, IUMA, University of Zaragoza, Zaragoza, Spain

ARTICLE INFO

MSC:
35B25
35B50
35K51
35K57
65L70
65M12
65M15
65M22
65M50

Keywords:
Singularly perturbed systems
Two-parameter problems
Large time delay
Numerical approximation
Scientific applications
High-order accuracy

ABSTRACT

A numerical method, used for solving two-parameter singularly perturbed systems with large time delays which are commonly encountered in a variety of scientific and engineering applications, is constructed and analyzed in this work. To attain high precision and stability, the suggested approach combines the cubic spline interpolation with the Crank–Nicolson method. The two-parameter nature of the problem introduces significant challenges due to the presence of boundary layers and the interaction of small perturbation parameters with large time delays. The technique successfully captures the abrupt changes and steep slopes present in such systems by using cubic splines. According to theoretical analysis, the suggested scheme significantly outperforms current techniques by achieving second-order convergence in both spatial and temporal variables. The theoretical conclusions are corroborated in practice by numerical experiments, which show the method's robustness and its efficiency. Discussions of applications in fluid dynamics, heat transport and control systems reflect clearly the approach's applicability in real-world scenarios. The findings show that the Crank–Nicolson method together with the cubic spline approach is an effective technique for precisely resolving two-parameter singularly perturbed systems with significant time delays, providing a solid foundation for practical scientific and engineering problems.

1. Introduction

Numerous real-world systems evolve across a variety of time frames due to their slow and rapid dynamics. These systems are singularly perturbed because they usually contain minor perturbations (small parameters) terms that multiply the highest-order derivative terms. Large time delays further complicate these systems, necessitating the use of specialized numerical techniques to find a correct numerical approximation [1,2]. Numerous scientific and technical applications, such as chemical reactor dynamics, brain signal transmission, climate modeling, power system stability and epidemiology, include singularly perturbed systems with two parameters. These applications cover multi-scale behavior, in which temporal delays are caused by transport lags, feedback control loops, or incubation periods, diffusion and response processes take place on different timescales. The stability and accuracy of the numerical approximations are greatly impacted by the existence of both a substantial time delay and a small perturbation parameter that multiplies the highest-order derivatives. These systems are characterized by singularly perturbed partial differential equations (PDEs) with two positive parameters (one for the second-order spatial derivative and another for the first-order spatial

* Corresponding author.
E-mail addresses: parvin.kumari@jaipur.manipal.edu (P. Kumari), clavero@unizar.es (C. Clavero).

https://doi.org/10.1016/j.matcom.2025.09.001
Received 10 April 2025; Received in revised form 1 September 2025; Accepted 3 September 2025
Available online 10 September 2025

derivative), which can be sufficiently small and also of different magnitude. Large time delays, such as the average process time of a control loop, can cause boundary layers, oscillations and negatively impact system stability. Because analytical solutions for these systems are uncommon, numerical approximation approaches play a crucial role in their study.

In this paper, we present a spline-based numerical approximation for solving a type of two-parameter singularly perturbed PDE systems with a significant time delay. The Crank–Nicolson finite difference method is used for the time discretization to assure stability and accuracy, whilst a cubic spline-based approach is used for the spatial discretization to efficiently capture abrupt gradients and boundary layers. The suggested method guarantees high accuracy in resolving boundary layers and capturing delayed effects effectively. This research aims to add to the numerical treatment of singularly perturbed systems with delays by providing insights into their stability, behavior and real-world consequences. Here are mathematical models for two-parameter singularly perturbed systems with large time delays in various real-world applications. Each model uses modest perturbation parameters to multiply first and second-order derivative components, as well as a large delay term.

Climate–Atmosphere Interaction with Heat Transport Delay: Analyzing ocean–atmosphere heat exchange with delayed effects [3].

$$\frac{\partial T_a}{\partial t} + \epsilon_1 \frac{\partial^2 T_a}{\partial x^2} + \epsilon_2 \frac{\partial T_a}{\partial x} + kT_a = h(T_o(t-\tau) - T_a),$$

$$\frac{\partial T_o}{\partial t} + \epsilon_1 \frac{\partial^2 T_o}{\partial x^2} + \epsilon_2 \frac{\partial T_o}{\partial x} + \gamma T_o = Q - h(T_o - T_a), \tag{1.1}$$

where:

- $T_a(x,t)$ is “atmospheric temperature”,
- $T_o(x,t)$ is “oceanic temperature”,
- ϵ_1 represents slow diffusion of heat,
- ϵ_2 models fast atmospheric response,
- k, γ are heat dissipation coefficients,
- h is the heat exchange parameter,
- Q represents external forcing,
- τ accounts for time delay in heat transport.

Epidemic Spread with Incubation Period Delay: Examining disease spread with incubation delays and spatial diffusion [4].

$$\frac{\partial S}{\partial t} + \epsilon_1 \frac{\partial^2 S}{\partial x^2} + \epsilon_2 \frac{\partial S}{\partial x} = -\beta S I(t-\tau),$$

$$\frac{\partial I}{\partial t} + \epsilon_1 \frac{\partial^2 I}{\partial x^2} + \epsilon_2 \frac{\partial I}{\partial x} = \beta S I(t-\tau) - \gamma I,$$

where:

- $S(x,t)$ is the susceptible population,
- $I(x,t)$ is the infected population,
- ϵ_1 represents slow diffusion of the disease,
- ϵ_2 models fast infection response,
- β is the transmission rate,
- γ is the recovery rate,
- τ represents the incubation period delay.

Species Competition with Migration and Delayed Growth: Two-parameter singularly perturbed systems with large time delays occur in ecological modeling, notably in species movement and competition scenarios. These models aid in understanding species cohabitation, habitat fragmentation, and population stability in dynamic situations. The existence of minor perturbation factors impacting both diffusion and response terms, combined with a lengthy time delay, results in complicated boundary layer behavior, necessitating numerical approximations [5].

$$\frac{\partial N_1}{\partial t} + \epsilon_1 \frac{\partial^2 N_1}{\partial x^2} + \epsilon_2 \frac{\partial N_1}{\partial x} = r_1 N_1(t-\tau)\left(1 - \frac{N_1 + \alpha N_2}{K_1}\right) - d_1 N_1 + M_1(N_1' - N_1),$$

$$\frac{\partial N_2}{\partial t} + \epsilon_1 \frac{\partial^2 N_2}{\partial x^2} + \epsilon_2 \frac{\partial N_2}{\partial x} = r_2 N_2(t-\tau)\left(1 - \frac{N_2 + \beta N_1}{K_2}\right) - d_2 N_2 + M_2(N_2' - N_2),$$

where:

- $N_1(x,t)$, $N_2(x,t)$ are population densities of two competing species,
- ϵ_1 represents slow migration across habitats,
- ϵ_2 is a small perturbation parameter affecting temporal growth,
- r_1, r_2 are intrinsic growth rates,

- K_1, K_2 are habitat carrying capacities,
- α, β are interspecies competition coefficients,
- d_1, d_2 are mortality rates,
- τ represents the reproduction delay (e.g., maturation period),
- M_1, M_2 are migration coefficients,
- N_1', N_2' represent populations in adjacent habitats.

The equation system shown above depicts the intricate interplay between species movement, competition and delayed reproduction. The inclusion of two minor perturbation parameters (ϵ_1 and ϵ_2) creates boundary layers, necessitating specialized numerical approaches to obtain efficient solutions. The substantial time delay (τ) refers to biological processes including gestation, maturation and delayed reaction to environmental changes, which impact species survival and coexistence. The diffusion parameters represent geographical dispersal, which is an important element in ecosystems facing habitat fragmentation or climate-induced migration. Unlike traditional Lotka–Volterra models, this approach takes into account both geographical and temporal heterogeneities, making it extremely useful for ecological conservation, invasive species management and epidemiological investigations. Because of the stiffness of the equations and the existence of boundary layers, traditional numerical approaches fail to produce stable solutions. As a result, the Crank–Nicolson technique (for the time discretization) is combined with the cubic spline collocation (for the spatial discretization) to obtain high-accuracy approximations while successfully resolving abrupt gradients at domain borders.

In [6] the authors proposed an adaptive approach for semilinear parabolic problems with singular perturbations. Their methodology merged Newton's method with adaptive discretization, which made use of a spatial finite element method and the backward Euler time-stepping system. They developed a strong a posteriori error analysis and created a completely adaptable Newton–Galerkin time-stepping method, showing its usefulness through numerical tests. A hybrid approach for singularly perturbed systems of second-order reaction–diffusion equations was presented in [7]. The authors used a numerical approach based on finite differences in conjunction with the Successive Complementary Expansion Method (SCEM). Examples demonstrating convergence features demonstrate how well their method approached solutions of singularly perturbed reaction–diffusion systems. In [8] the authors improved the accuracy of capturing boundary layer behaviors by creating a fitted mesh B-spline collocation technique for singularly perturbed differential–difference equations with large delays. In [9], they introduced a parameter-uniform numerical technique for singularly perturbed partial differential equations with time lag, assuring uniform convergence across perturbation parameters. A numerical technique for singularly perturbed parabolic time delay convection–diffusion–reaction equations was proposed in [10]. The authors used the Crank–Nicolson approach for temporal discretization in conjunction with an exponentially fitted operator finite difference method. Their method handled boundary layers and time delays well, achieving uniform convergence without limiting mesh production.

An effective hybrid numerical technique for tackling coupled systems of singularly perturbed linear parabolic problems was constructed in [11]. The approach coupled a high-order hybrid scheme on a generalized Shishkin mesh for spatial discretization with an additive system for temporal discretization. With first-order precision in time and third-order accuracy in space, the authors presented an error analysis showing uniform convergence. Recently, an effective numerical method for singularly perturbed time-delayed parabolic problems with two parameters was introduced in [12]. They used a fitted numerical approach to deal with the difficulties caused by temporal delays and tiny perturbation parameters, obtaining parameter-uniform convergence and using numerical experiments to show the method's efficacy. In [13] it was analyzed a system of time-dependent singularly perturbed differential–difference equations characterized by small shifts, using Taylor series expansions and a combination of the Crank–Nicolson method with a Shishkin-type mesh and cubic B-spline collocation method, achieving nearly second-order accuracy. The numerical approximation of first-order linear and nonlinear singularly perturbed initial value linked systems was examined in [14]. They did this by combining the backward differences with a suitable component splitting in two effective discretization techniques. In [15] a 2D elliptic singularly perturbed system was considered, where the diffusion parameters are the same and the convection parameters are also the same, similarly to problem (1.2) considered here. In [16] that work was extended to the case where the diffusion parameters can be different and in [17,18] to the most general case for which both the diffusion and the convection parameters can be all different In all those works, uniformly convergent methods, based on the classical upwind scheme, were constructed on adequate Shishkin meshes for the different cases.

In this work, we consider a 1D system of singularly perturbed delay parabolic IBVP on $\mathcal{M} = \mathcal{M}_x \times \mathcal{M}_s = (0,1) \times (0,\mathrm{S}]$ given by

$$\mathcal{L}\mathbf{X} := \frac{\partial \mathbf{X}}{\partial s} + \mathcal{L}_{x,\nu_1,\nu_2}\mathbf{X} = -a(x)\mathbf{X}(x, s-\tau) + \mathbf{f}(x,s), \ (x,s) \in \mathcal{M}, \tag{1.2a}$$

$$X(0,s) = \mathfrak{l}(s) \text{ in } \mathcal{M}_l, \quad \mathbf{X}(1,s) = \mathfrak{m}(s) \text{ in } \mathcal{M}_r, \quad \mathbf{X}(s,0) = \boldsymbol{\psi} \text{ in } \mathcal{M}_b, \tag{1.2b}$$

where $\mathcal{M}_l = \{(0,s)|\ 0 \le s \le \mathrm{S}\}$, $\mathcal{M}_r = \{(1,s)|\ 0 \le s \le \mathrm{S}\}$, $\mathcal{M}_b = \overline{\mathcal{M}}_x \times \Lambda^* = [0,1] \times (-\tau, 0]$, and $\mathcal{L} = (\mathcal{L}_1, \mathcal{L}_2)^T$. Further, the operators $\mathcal{L}_{x,\nu_1,\nu_2}$ and $\mathcal{L}_i$, for $i = 1,2$, are defined as

$$\mathcal{L}_{x,\nu_1,\nu_2} = -\mathrm{E}_1 \frac{\partial^2}{\partial x^2} - \mathrm{E}_2 P(x) \frac{\partial}{\partial x} + Q(x,s),$$

$$\mathcal{L}_i\mathbf{X} = \frac{\partial X_i}{\partial s} - \nu_1 \frac{\partial^2 X_i}{\partial x^2} - \nu_2 p_{kk}(x) \frac{\partial X_i}{\partial x} + \sum_{j=1}^{2} q_{ij}(x,s) X_j,$$

where $E_1 = \begin{pmatrix} \nu_1 & 0 \\ 0 & \nu_1 \end{pmatrix}$, $E_2 = \begin{pmatrix} \nu_2 & 0 \\ 0 & \nu_2 \end{pmatrix}$, $P(x) = \begin{pmatrix} p_{11}(x) & 0 \\ 0 & p_{22}(x) \end{pmatrix}$, $Q(x,s) = \begin{pmatrix} q_{11}(x,s) & q_{12}(x,s) \\ q_{21}(x,s) & q_{22}(x,s) \end{pmatrix}$, $\mathbf{f}(x,s) = (f_1(x,s), f_2(x,s))^T$, $\mathbf{X}(x,s) = (X_1(x,s), X_2(x,s))^T$, $\mathfrak{l}(s) = (\mathfrak{l}_1(s), \mathfrak{l}_2(s))^T$, $\mathfrak{m}(s) = (\mathfrak{m}_1(s), \mathfrak{m}_2(s))^T$. For each $(x,s) \in \overline{\mathcal{M}}$ and $x \in \overline{\mathcal{M}}_x$, the matrices $P(x)$ and $Q(x,s)$ satisfy

$$p_{jj}(x) \geq \alpha_j > 0, \ \ j = 1,2, \tag{1.3a}$$

$$Q(x,s) \text{ is an } L_0 \text{ matrix} \Rightarrow \ \ q_{jk}(x,s) \leq 0, j \neq k, \ q_{kk} > 0, \ \ j,k = 1,2, \tag{1.3b}$$

$$\sum_{k=1}^{2} q_{jk}(x,s) \geq \Phi > 0, q_{ii}(x,s) > |q_{ij}(x,s)|, \ \ i,j = 1,2. \tag{1.3c}$$

Here, we denote by $\alpha = \min\{\alpha_1, \alpha_2\}$ and $\eta = \min_{(x,s)\in\overline{\mathcal{M}}} \left\{ \dfrac{q_{i1}(x,s) - q_{i2}(x,s)}{p_{ii}(x)} \right\}$, $i = 1,2$.

These conditions guarantee the presence of a boundary layer in both solution components at $x = 1$. Additionally, sufficient compatibility conditions are assumed on the data of the continuous problem at the corner locations $(0,0)$ and $(1,0)$, in order that the posterior developments are valid. The first ones of those compatibility conditions are given by

$$\begin{cases} \boldsymbol{\phi}(0,0) = \boldsymbol{\phi}_l(0), \ \ \boldsymbol{\phi}(1,0) = \boldsymbol{\phi}_r(0), \\ \dfrac{d\boldsymbol{\phi}_l(0)}{ds} - \nu_1 \dfrac{\partial^2 \boldsymbol{\phi}(0,0)}{\partial x^2} - \nu_2 p_{11}(0,0) \dfrac{\partial \boldsymbol{\phi}(0,0)}{\partial x} + q_{11}(0,0)\boldsymbol{\phi}(0,0) + q_{12}(0,0)\boldsymbol{\phi}(0,0) = -a(0)\boldsymbol{\phi}(0,-\tau) + \mathbf{f}(0,0), \\ \dfrac{d\boldsymbol{\phi}_r(0)}{ds} - \nu_1 \dfrac{\partial^2 \boldsymbol{\phi}(1,0)}{\partial x^2} - \nu_2 p_{11}(1,0) \dfrac{\partial \boldsymbol{\phi}(1,0)}{\partial x} + q_{21}(1,0)\boldsymbol{\phi}(1,0) + q_{22}(1,0)\boldsymbol{\phi}(1,0) = -a(1)\boldsymbol{\phi}(1,-\tau) + \mathbf{f}(1,0). \end{cases} \tag{1.4}$$

Previous compatibility conditions, are the extension of those ones for the scalar case (see [19]), which have been expanded in this study.

Two-parameter singular perturbation BVPs are used to describe boundary layer phenomena in fluid dynamics, where high Reynolds or Peclet numbers cause fast changes near the boundaries. These problems are crucial in comprehending viscous movements and heat transfer in fluids [20]. Chemical engineers utilize reaction–diffusion systems with two small parameters to represent processes where diffusion and reaction rates interact, resulting in abrupt gradients or layers in concentration profiles [21,22]. The problem (1.2) may be classified into two groups based on the parameter ν_1 and ν_2. When $\nu_2 = 1$, the problem under discussion belongs to the one-parameter time-dependent convection–diffusion PDE class, and a boundary layer with a width of $\mathcal{O}(\nu_1)$ is visible in the neighborhood of $x = 0$. Both ends, $x = 0$ and $x = 1$, have two boundary layers, each having a width of $\mathcal{O}(\sqrt{\nu_1})$, in the case that $\nu_2 = 0$. Except for these two cases ($\nu_2 \neq 0, 1$), the ratio of ν_2^2 to ν_1 produces two unique outcomes in our two-parameter PDE. At $x = 0$ and $x = 1$, two boundary layers are visible; these two cases are associated to the ratio $\dfrac{\nu_2^2}{\nu_1} \ll 1$ or $\dfrac{\nu_2^2}{\nu_1} \gg 1$, $\nu_2 = 1$, respectively.

Benefits of spline techniques: When it comes to addressing singularly perturbed problems with delays and other difficult numerical circumstances, spline approaches have the following advantages:

- Splines provide solutions at any point within the region of interest, offering greater flexibility and accuracy than methods that only provide solutions at discrete grid points.
- Splines can efficiently approximate solutions for differential equations with boundary and interior layers.
- They can be adapted for problems with non-uniform grids, such as Shishkin-type meshes, to resolve sharp gradients.
- Splines are useful for approximation (fitting a smooth curve around the data points) as well as interpolation (passing through specified data points).
- The method's simplicity helps to reduce the problem's overall complexity and computation expense. The system's tridiagonal coefficient matrix simplifies computation and reduces the overall complexity of the equation system.

So, spline approaches provide a mix of computing efficiency, flexibility and smoothness, making them effective tools for modeling and analyzing complicated shapes and functions. Their wide range of applications and robust mathematical foundations make them are very convenient in many fields.

Up our knowledge, there are not previous works where uniformly convergent numerical methods, having second order in time and almost second order in space, are studied, when they were used to approximate the exact solution of one-dimensional parabolic singularly perturbed systems, for which there are small parameters in both the diffusion and the convection terms. This is the main contribution of the present work.

This paper is organized like this. The appropriate a priori asymptotic behavior of the exact solution of the continuous problem is presented in Section 2. In particular, we prove the maximum principle and also adequate bounds for the solution and its derivatives. Bounds for both smooth and singular components are provided by breaking down the solution into its constituent parts. A discrete numerical method for solving the continuous problem is presented in Section 3. In order to assess the correctness of the technique, Section 4 focused on obtaining parameter-uniform error estimates. Section 5 discusses and shows the numerical results obtained for two test examples that validate in practice the theoretical conclusions. Lastly, Section 6 presents some conclusions.

2. Asymptotic behavior of the exact solution

In this section, we prove which is the asymptotic behavior of the exact solution with respect to the diffusion and the convection parameters. Also, we give an adequate decomposition of the exact solution in its regular and singular components, proving appropriated bounds for its partial derivatives, which will be useful in the posterior analysis of the uniform convergence of the numerical method used to solve the continuous problem.

Lemma 2.1. *Let* $\mathbf{X} \in (C^{(2,1)}(\mathcal{M}) \cap C^{(0,0)}(\overline{\mathcal{M}}))^2$ *so that* $\mathbf{X} \geq \mathbf{0}$ *on* Λ ($\Lambda = \mathcal{M}_l \cup \mathcal{M}_r \cup \mathcal{M}_b$). *Then* $\mathcal{L}\mathbf{X} \geq \mathbf{0}$, $\forall (x,s) \in \mathcal{M}$ *provides* $\mathbf{X} \geq \mathbf{0}$, $\forall (x,s) \in \overline{\mathcal{M}}$.

Proof. The procedures outlined in [13] can be used to complete the proof. □

Lemma 2.2. *The following inequality proves the stability bound for* $\mathbf{X}$ *in* (1.2).

$$\|\mathbf{X}\|_{\overline{\mathcal{M}}} \leq \frac{1}{\alpha}\|\mathbf{f}\|_{\overline{\mathcal{M}}} + \max\{\|\mathfrak{l}\|_{\overline{\mathcal{M}_s}}, \|\mathfrak{m}\|_{\overline{\mathcal{M}_s}}\}.$$

Proof. We begin by taking the barrier function $\boldsymbol{\phi}^{\pm}(x,s) = \frac{1}{\alpha}\|\mathbf{f}\|_{\overline{\mathcal{M}}} + \max\{\|\mathfrak{l}\|_{\overline{\mathcal{M}_s}}, \|\mathfrak{m}\|_{\overline{\mathcal{M}_s}}\}\mathbf{X}(x,s)$, $(x,s) \in \overline{\mathcal{M}}$, Afterward, use Lemma 2.1 to get the desired outcome. □

Lemma 2.3. *The following time derivative requirements are satisfied by the solution* $\mathbf{X}$ *of* (1.2).

$$\left\| \frac{\partial^i \mathbf{X}}{\partial s^i} \right\|_{\overline{\mathcal{M}}} \leq C, \quad i = 0, 1, 2.$$

Proof. To prove the result, we first use the barrier function $\boldsymbol{\phi} = \mathbf{C}(1+s)$. Let $\mathbf{S} = \mathbf{X}_s$, we start with $\mathbf{X}_s$. On $\mathcal{M}_l \cup \mathcal{M}_r$; $\mathbf{S}$ fulfills

$$|\mathbf{S}(x,s)| \leq \max_{s \in \overline{\mathcal{M}_s}} \{|\mathfrak{l}'_s|, |\mathfrak{m}'_s|\} \leq \mathbf{C}.$$

In $\overline{\mathcal{M}}_x$, we know that $X_i(x,0) = 0$ at $s = 0$ for all x which gives $\dfrac{\partial X_i(x,0)}{\partial x} = 0$, also $\forall\, x \in \overline{\mathcal{M}}_x$, $\dfrac{\partial^2 X_i(x,0)}{\partial x^2} = 0$. Eq. (1.2a) gives

$$\frac{\partial X_i(x,0)}{\partial s} = f_i(x,0) + \nu_1 \frac{\partial^2 X_i(x,0)}{\partial x^2} + \nu_2 p_{ii} \frac{\partial X_k(x,0)}{\partial x} - \sum_{j=1}^{2} q_{kj}(x,0) X_j(x,0),$$

which provides

$$\|\mathbf{S}(x,0)\|_{\overline{\mathcal{M}}_x} = \|\mathbf{f}(x,0)\|_{\overline{\mathcal{M}}_x} \leq C.$$

When differentiating Eq. (1.2a) with respect to s, we get

$$\mathcal{L}\mathbf{S} = \mathbf{f}_s - D_s\mathbf{X}, \ (x,s) \in \mathcal{M},$$

where $D_s = \left(\frac{\partial q_{ij}}{\partial s}\right)$. Also $\|\mathbf{S}\|_{\overline{\mathcal{M}}} = \|\mathbf{X}_s\|_{\overline{\mathcal{M}}} \leq C$, applying the same barrier function as before. The analysis for $\mathbf{T} = \mathbf{X}_{ss}$ is shown below.

$$|\mathbf{T}(x,s)| \leq \mathbf{C}, \quad (x,s) \in \mathcal{M}_l \cup \mathcal{M}_r,$$
$$\|\mathbf{T}(x,0)\|_{\overline{\mathcal{M}}_s} = \|\mathbf{f}_s(x,0) - D_s\mathbf{X} - \mathcal{L}_{x,\nu_1,\nu_2}\mathbf{f}(x,0)\|_{\overline{\mathcal{M}}_x} \leq C,$$
$$\mathcal{L}\mathbf{T} = \mathbf{f}_{ss} - D_{ss}\mathbf{X} - 2D_s\mathbf{X}_s, \ (x,s) \in \mathcal{M},$$

where $D_{ss} = \left(\frac{\partial^2 q_{ij}}{\partial s^2}\right)$. Then, by repeatedly employing $\boldsymbol{\phi} = \mathbf{C}(1+s)$, $\|\mathbf{T}\|_{\overline{\mathcal{M}}} = \|\mathbf{X}_{ss}\|_{\overline{\mathcal{M}}} \leq C$ is obtained which is the required result. □

Lemma 2.4. *The derivatives of the solution satisfy the following estimations for* $l, m \in \{0,1,2,3,4\}$ *with* $0 \leq l + 2\,m \leq 4$.

$$\left\| \frac{\partial^{l+m}\mathbf{X}}{\partial s^l \partial x^m} \right\| \leq C \begin{cases} \dfrac{1}{(\sqrt{\nu_1})^m}, & \text{if } \alpha\nu_2^2 \leq \eta\nu_1, \\ \left(\dfrac{\nu_2}{\nu_1}\right)^m \left(\dfrac{\nu_2^2}{\nu_1}\right)^l, & \text{if } \alpha\nu_2^2 \geq \eta\nu_1. \end{cases}$$

Proof. To illustrate the outcomes, we look at two different scenarios: $\alpha\nu_2^2 \geq \eta\nu_1$ and $\alpha\nu_2^2 \leq \eta\nu_1$. The stretched variable $\hat{x} = \dfrac{x}{\sqrt{\nu_1}}$ is obtained by altering Eq. (1.2) for the variable x, which corresponds to $\alpha\nu_2^2 \leq \eta\nu_1$. Let $\widehat{\mathcal{T}} = (0,T) \times \left(0, \dfrac{1}{\sqrt{\nu_1}}\right)$ and $\partial\widehat{\mathcal{M}}$ is the extent of $\widehat{\mathcal{M}}$ that is associated with $\partial\mathcal{M}$.

The step techniques and the result in ([19], Theorem 10.1) are now used to establish the following limits for $l, m \in \{0, 1, 2, 3, 4\}$ with $0 \leq l + 2\ m \leq 4$. Then, it holds

$$\left\| \frac{\partial^{l+m}\mathbf{X}}{\partial s^l \partial x^m} \right\|_{W_{\gamma,\xi}} \leq C(1 + \|\hat{\mathbf{X}}\|_{\overline{\hat{\mathcal{M}}}}),$$

where, for each $\xi \in \left(0, \frac{1}{\sqrt{\nu_1}}\right)$ and $\gamma > 0$, $W_{\gamma,\xi} = ((0, \mathrm{S}] \times (\xi - \gamma, \xi + \gamma)) \cap \hat{\mathcal{M}}$. In order to accomplish our objective, we return to the initial variable.

Once the stretched variables $\tilde{x} = \frac{\nu_2 x}{\nu_1}$ and $\tilde{s} = \frac{\nu_2^2 s}{\nu_1}$ have been taken into consideration, we are left with the following problem:

$$\begin{cases} -\tilde{\mathbf{X}}_{\tilde{x}\tilde{x}} - \tilde{\mathcal{P}}\tilde{\mathbf{X}}_{\tilde{x}} - \frac{\nu_1}{\nu_2^2}\tilde{\mathcal{Q}}\tilde{\mathbf{X}} + \tilde{\mathbf{X}}_{\tilde{s}} = \tilde{\mathbf{f}}, \text{in } \tilde{\mathcal{M}}, \\ \tilde{\mathbf{X}}|_{\tilde{\mathcal{M}}_l} = \tilde{\mathrm{l}},\ \tilde{\mathbf{X}}|_{\tilde{\mathcal{M}}_r} = \tilde{\mathrm{m}},\ \tilde{\mathbf{X}}|_{\tilde{\mathcal{M}}_b} = \tilde{\boldsymbol{\psi}}, \end{cases}$$

for $\alpha\nu_2^2 \geq \eta\nu_1$, where $\widetilde{\mathcal{M}} = \left(0, \mathrm{s}\frac{\nu_2^2}{\nu_1}\right] \times \left(0, \frac{\nu_2}{\nu_1}\right)$ and $\partial\tilde{\mathcal{M}}$ is the boundary of $\tilde{\mathcal{M}}$ that corresponds to $\partial\mathcal{M}$. Until we get the desired outcome, we continue to follow the same procedures as before. □

Previous bounds for the derivatives do not show the presence of boundary layer in the exact solution and they are not sufficient for the analysis of the uniform convergence of the numerical method defined posteriorly. To obtain precise estimates, we need to decompose the exact solution $\mathbf{X}$ into its regular and layer components. This decomposition is given in the form

$$\mathbf{X} = \underbrace{\mathbf{X}_r}_{\text{regular component}} + \underbrace{\mathbf{X}_L}_{\text{left layer component}} + \underbrace{\mathbf{X}_R}_{\text{right layer component}},$$

where the components are the solution of the problems

$$\begin{cases} \mathcal{L}\mathbf{X}_r = \mathbf{f}(x, s), \quad \mathbf{X}_r(x, 0), \quad \mathbf{X}_r(x, 1) \text{ chosen suitably}, \quad \mathbf{X}_r(x, s)|_{\mathcal{M}_b} = \boldsymbol{\psi}, \\ \mathcal{L}\mathbf{X}_L = \mathbf{0},\ \mathbf{X}_L|_{\mathcal{M}_l} = \mathbf{X} - \mathbf{X}_r - \mathbf{X}_R, \quad \mathbf{X}_L|_{\mathcal{M}_r} \text{ chosen suitably}, \ \mathbf{X}_L(x, s)|_{\mathcal{M}_b} = \boldsymbol{\psi}, \\ \mathcal{L}\mathbf{X}_R = \mathbf{0}, \mathbf{X}_R|_{\mathcal{M}_r} = \mathbf{X} - \mathbf{X}_r - \mathbf{X}_L, \quad \mathbf{X}_R|_{\mathcal{M}_l} \text{ chosen suitably}, \ \mathbf{X}_R(x, s)|_{\mathcal{M}_b} = \boldsymbol{\psi}. \end{cases} \tag{2.1}$$

Lemma 2.5. *The layer components $\mathbf{X}_L$, $\mathbf{X}_R$ satisfy the bounds*

$$|\mathbf{X}_L(x, s)| \leq C \exp(-\theta_1 x), \quad |\mathbf{X}_R(x, s)| \leq C \exp(-\theta_2(1 - x)),$$

where

$$\theta_1 = \begin{cases} \frac{\sqrt{\eta\alpha}}{\sqrt{\nu_1}}, & \text{if } \alpha\nu_2^2 \leq \eta\nu_1, \\ \frac{\alpha\nu_2}{\nu_1}, & \text{if } \alpha\nu_2^2 \geq \eta\nu_1, \end{cases} \qquad \theta_2 = \begin{cases} \frac{\sqrt{\eta\alpha}}{2\sqrt{\nu_1}}, & \text{if } \alpha\nu_2^2 \leq \eta\nu_1, \\ \frac{\eta}{2\nu_2}, & \text{if } \alpha\nu_2^2 \geq \eta\nu_1. \end{cases}$$

Proof. Make use of the barrier functions $\Phi^{\pm}(x, s) = C \exp(-\theta_1 x) \pm \mathbf{X}_L(x, s)$ to obtain $|\mathbf{X}_L(x, s)|$'s necessary bound. The proof for $|\mathbf{X}_R(x, s)|$ is very similar to that for $\alpha\nu_2^2 \leq \eta\nu_1$. Suppose $\Phi^{\pm}(x, s) = C \exp\left(-\frac{\sqrt{\eta\alpha}}{2\sqrt{\nu_1}}(1 - x)\right) \pm \mathbf{X}_L(x, s)$ for the case $\alpha\nu_2^2 \geq \eta\nu_1$ and use the maximum principle to obtain the required result and refer [23] for more details. □

3. Discretization and numerical method

3.1. Time-dependent discretization

In this part, we provide an approach for determining the Interpolation/Extrapolation points, which are necessary to define $s - \tau$ in terms of the computational grid points and also to calculate $\mathbf{X}(x, s - \tau)$.

The steps of the algorithm are as follows:

1. For a given $\mathcal{N}_s$, define the set $\Omega_s^{\mathcal{N}_s}$ as:

$$\Omega_s^{\mathcal{N}_s} = \{s_{\mathrm{n}} = \mathrm{n}\Delta s \mid \mathrm{n} = 0, 1, \ldots, \mathcal{N}_s\}.$$

2. Assign a value to τ.
3. Set the function $\mathbf{X}(x,s)$ using the interval and boundary conditions:

$$\mathbf{X}(x,s) = \boldsymbol{\phi}(x,s), \quad -\tau \le s \le 0,$$

$$\mathbf{X}(0,s) = \mathfrak{l}(s), \quad \mathbf{X}(1,s) = \mathfrak{m}(s).$$

4. Determine the non-negative integer K as

$$\mathrm{K} = \lfloor \tau/\Delta s \rfloor,$$

where $\lfloor p \rfloor$ represents the floor function of p.
5. For any $s_{\mathfrak{m}}$ in the subset $\{s_{\mathfrak{n}}\}_{\mathfrak{n}=1}^{\mathrm{K}}$, which belongs to the range $0 < s \le \tau$, it follows that $s_{\mathfrak{n}} - \tau \in (-\tau, 0]$. Hence, we can substitute $\mathbf{X}(x, s-\tau)$ with $\boldsymbol{\phi}(x, s-\tau)$ based on the interval condition.
6. For any $s_{\mathfrak{l}} \in \{s_{\mathfrak{n}}\}_{\mathfrak{n}=\mathrm{K}+1}^{\mathcal{N}_s-1}$, which corresponds to $\tau < s < 1$, we observe that $s-\tau$ falls within the interval $[s_{\mathfrak{l}-\mathrm{K}-1}, s_{\mathfrak{l}-\mathrm{K}}]$.
7. Express the delayed term $s-\tau$ as a weighted combination of $s_{\mathfrak{l}-\mathrm{K}-1}$ and $s_{\mathfrak{l}-\mathrm{K}}$:

$$s - \tau = \eth s_{\mathfrak{l}-\mathrm{K}-1} + (1-\eth) s_{\mathfrak{l}-\mathrm{K}}, \quad \mathrm{K}+1 \le \mathfrak{l} < \mathcal{N}_s,$$

where the weighting factor $\eth$ is given by

$$\eth = \frac{s_{\mathfrak{l}-\mathrm{K}} - s_{\mathfrak{l}} + \tau}{\Delta s} \ge 0.$$

8. Finally, we approximate $\mathbf{X}(x, s-\tau)$ using linear interpolation without affecting the validity of our conclusions:

$$\mathbf{X}(x, s-\tau) = \eth \mathbf{X}(x,s)_{\mathfrak{l}-\mathrm{K}-1} + (1-\eth)\mathbf{X}(x, s_{\mathfrak{l}-\mathrm{K}}), \quad \mathrm{K}+1 \le \mathfrak{l} < \mathcal{N}_s.$$

Note 1. If $\tau < \Delta s$, then $\mathrm{K} = \lfloor \frac{\tau}{\Delta s} \rfloor = 0$, which implies that $s-\tau$ lies in the interval $(s_{\mathfrak{m}-1}, s_{\mathfrak{l}})$. In this case, we determine $s-\tau$ by interpolating between the nodes $s_{\mathfrak{l}}$ and $s_{\mathfrak{l}-1}$.

Note 2. If $\tau > 0$ and $s-\tau$ belongs to the set $\bar{\Omega}_s^{\mathcal{N}_s}$, then there exists an index K such that $s - \tau = s_{\mathfrak{l}-\mathrm{K}}$. This results in $\eth = 0$, meaning no interpolation or extrapolation is needed. However, in general, $s_{\mathfrak{l}} - \tau$ does not necessarily belong to $\bar{\Omega}_s^{\mathcal{N}_s}$.

We use the Crank–Nicolson discretization, which is renowned for its implicit formulation and second-order accuracy, to discretize in time on a uniform mesh. Because of its improved stability features, this method is especially beneficial for stiff difficulties. At the $(\mathfrak{m}+\frac{1}{2})$th time level, the discretized form of Eq. (1.2) may be written as

$$\widetilde{\boldsymbol{X}}^{\mathfrak{n}+1}(x) = \boldsymbol{\phi}(x, s_{\mathfrak{n}+1}),\ x \in \Omega_b, (-\mathrm{K}+1) \le \mathfrak{n} < 0, \tag{3.1a}$$

$$\mathbb{L}\widetilde{\boldsymbol{X}}^{\mathfrak{n}+1}(x) = -\frac{\mathrm{E}_1}{2}\widetilde{\boldsymbol{X}}_{xx}^{\mathfrak{n}+1}(x) - \mathrm{E}_2 \frac{P^{\mathfrak{n}+\frac{1}{2}}(x)}{2}\widetilde{\boldsymbol{X}}_{x}^{\mathfrak{n}+1}(x) + \left(\frac{1}{\Delta s} I + \frac{Q^{\mathfrak{n}+\frac{1}{2}}(x)}{2}\right)\widetilde{\boldsymbol{X}}^{\mathfrak{m}+1}(x) = -a^{\mathfrak{n}+1}(x)\widetilde{\boldsymbol{X}}^{\mathfrak{n}+1-\mathrm{K}} + \mathfrak{f}^{\mathfrak{n}+1}(x),$$

$$x \in \Omega_x,\ \mathfrak{n} \ge 0, \tag{3.1b}$$

$$\widetilde{\boldsymbol{X}}^{\mathfrak{n}+1}(0) = \mathfrak{l}(s_{\mathfrak{n}+1}),\ \widetilde{\boldsymbol{X}}^{\mathfrak{n}+1}(1) = \mathfrak{n}(s_{\mathfrak{n}+1}),\ \mathfrak{n} \ge 0, \tag{3.1c}$$

where I denotes the identity matrix of order 2×2, $P^{\mathfrak{n}+\frac{1}{2}}(x) = P(x)$, $Q^{\mathfrak{n}+\frac{1}{2}}(x) = (q_{ij}(x, s_{\mathfrak{n}+\frac{1}{2}}))_{1\le i,j\le 2}$, $\widetilde{\boldsymbol{X}}^{\mathfrak{n}+1} \approx \boldsymbol{X}(x, s_{\mathfrak{n}+1})$ represents the $(\mathfrak{n}+1)$th time level approximation of the solution to Eq. (3.1) and

$$\mathfrak{f}^{n+1}(x) = \boldsymbol{f}^{\mathfrak{n}+\frac{1}{2}}(x) + \frac{\mathrm{E}_1(x)}{2}\widetilde{\boldsymbol{X}}_{xx}^{\mathfrak{n}+1}(x) + \mathrm{E}_2\frac{P^{\mathfrak{n}+\frac{1}{2}}(x)}{2}\widetilde{\boldsymbol{X}}_{x}^{\mathfrak{n}+1}(x) + \left(\frac{1}{\Delta s} I - \frac{Q^{\mathfrak{n}+\frac{1}{2}}(x)}{2}\right)\widetilde{\boldsymbol{X}}^{\mathfrak{n}}(x).$$

The equation above may be rewritten as

$$\widetilde{\boldsymbol{X}}^{\mathfrak{n}+1}(x) = \boldsymbol{\phi}(x, s_{\mathfrak{n}+1}),\ x \in \Omega_b, (-\mathrm{K}+1) \le \mathfrak{n} < 0, \tag{3.2a}$$

$$\mathbb{L}\widetilde{\boldsymbol{X}}^{\mathfrak{n}+1}(x) = -\frac{\mathrm{E}_1(x)}{2}\widetilde{\boldsymbol{X}}_{xx}^{\mathfrak{n}+1}(x) - \mathrm{E}_2\frac{P^{\mathfrak{n}+\frac{1}{2}}(x)}{2}\widetilde{\boldsymbol{X}}_{x}^{\mathfrak{n}+1}(x) + \left(\frac{1}{\Delta s} I + \frac{Q^{\mathfrak{n}+\frac{1}{2}}(x)}{2}\right)\widetilde{\boldsymbol{X}}^{\mathfrak{n}+1}(x) = \grave{\boldsymbol{g}}^{\mathfrak{n}+1}(x),\ x \in \Omega_x,\ \mathfrak{n} \ge 0, \tag{3.2b}$$

$$\widetilde{\boldsymbol{X}}^{\mathfrak{n}+1}(0) = \mathfrak{l}(s_{\mathfrak{n}+1}),\ \widetilde{\boldsymbol{X}}^{\mathfrak{n}+1}(1) = \mathfrak{n}(s_{\mathfrak{n}+1}),\ \mathfrak{n} \ge 0, \tag{3.2c}$$

where

$$\grave{\boldsymbol{g}}^{\mathfrak{n}+1}(x) = -a^{\mathfrak{n}+1}(x)\widetilde{\boldsymbol{X}}^{\mathfrak{n}+1-\mathrm{K}} + \mathfrak{f}^{\mathfrak{n}+1}(x).$$

Eq. (3.2) is rewritten as follows for the components $\widetilde{X}_k^{\mathfrak{n}+1}$, where $k = 1, 2$:

$$\widetilde{\boldsymbol{X}}_k^{\mathfrak{n}+1}(x) = \boldsymbol{\phi}(x, s_{\mathfrak{n}+1}),\ x \in \Omega_b, (-\mathrm{K}+1) \le \mathfrak{n} < 0, \tag{3.3a}$$

$$\mathbb{L}_k\widetilde{\boldsymbol{X}}^{n+1}(x) \equiv -\frac{\nu_1}{2}(\widetilde{X}^{n+1}_{xx})_k(x) - \nu_2\frac{p_{kk}^{n+\frac{1}{2}}(x)}{2}(\widetilde{X}^{n+1}_{x})_k(x) + \left(\frac{1}{\Delta s} + \frac{q_{kk}^{n+\frac{1}{2}}(x)}{2}\right)\widetilde{X}^{n+1}_k(x),$$

$$+ \frac{q_{lk}^{n+\frac{1}{2}}(x)}{2}\widetilde{X}^{n+1}_l(x) = \hat{g}_k^{\,n+1}(x),\ l \neq k, \tag{3.3b}$$

$$\widetilde{X}^{n+1}_k(0) = \mathfrak{l}_k(s_{n+1}),\ \widetilde{X}^{n+1}_k(1) = \mathfrak{n}_k(s_{n+1}),\ n \geq 0, \tag{3.3c}$$

where

$$\hat{g}^{n+1}_k(x) = \mathfrak{f}_k^{n+\frac{1}{2}}(x) + \frac{\nu_1}{2}(\widetilde{X}^{n}_{xx})_k(x) + \nu_2\frac{p_{kk}^{n+\frac{1}{2}}(x)}{2}\widetilde{X}^{n}_k(x) + \left(\frac{1}{\Delta s} - \frac{q_{kk}^{n+\frac{1}{2}}(x)}{2}\right)\widetilde{X}^{n}_k(x) - \frac{q_{lk}^{n+\frac{1}{2}}(x)}{2}\widetilde{X}^{n}_l(x).$$

The local truncation error (LTE) may be examined with the help of the auxiliary problem

$$\mathbb{L}\widehat{\boldsymbol{X}}^{n+1}(x) \equiv -\frac{\mathrm{E}_1}{2}\widehat{\boldsymbol{X}}^{n+1}_{xx}(x) - \mathrm{E}_2\frac{P^{n+\frac{1}{2}}(x)}{2}\widehat{\boldsymbol{X}}^{n+1}_{x}(x) + \left(\frac{1}{\Delta s} + \frac{Q^{n+\frac{1}{2}}(x)}{2}\right)\widehat{\boldsymbol{X}}^{n+1}(x),$$

$$= \hat{\boldsymbol{g}}_k^{\,n+1}(x), \tag{3.4a}$$

$$\widehat{\boldsymbol{X}}^{n+1}(0) = \mathfrak{l}(s_{n+1}),\ \widehat{\boldsymbol{X}}^{n+1}(1) = \mathfrak{n}(s_{n+1}),\ n \geq 0, \tag{3.4b}$$

where the exact solution of the continuous problem at time level n replaces the numerical approximation $\widetilde{\boldsymbol{X}}^{n}(x)$ in (3.1) (see [1]).

Lemma 3.1. *The following definitions of LTE and global error are well known:*

$$\boldsymbol{\mathcal{E}}^{n+1} = \boldsymbol{X}(x, s_{n+1}) - \widehat{\boldsymbol{X}}^{n+1}(x),\ \boldsymbol{\mathcal{G}}^{n} = \boldsymbol{X}(x, s_{n+1}) - \widetilde{\boldsymbol{X}_k}^{n+1}(x).$$

Then, the following bounds hold

$$\|\boldsymbol{\mathcal{E}}^{n+1}\| \leq C(\Delta s)^3, \tag{3.5a}$$

$$\|\boldsymbol{\mathcal{G}}^{n}\| \leq C(\Delta s)^{3/2},\ n \leq \frac{\mathrm{T}}{\Delta s}. \tag{3.5b}$$

Proof. For readers interested in proof, see [1,24]. □

Remark 3.2. The order reduction in the convergence of the time discretization showed in the previous result is due to the study of its uniform stability, as it was proven in [1]. Nevertheless, as we will see in the numerical results section, this reduction is only from a theoretical point of view and it is not observed in practice.

Lemma 3.3. *The estimated solution $\widetilde{\boldsymbol{X}}^{n+1}$ in (3.1) may be broken down into its regular, left layer, and right layer components of the form*

$$\widetilde{\boldsymbol{X}}^{n+1}(x) = \widetilde{\boldsymbol{X}}^{n+1}_r(x) + \widetilde{\boldsymbol{X}}^{n+1}_L(x) + \widetilde{\boldsymbol{X}}^{n+1}_R(x),$$

just like in (2.1), so that

$$|(\widetilde{\boldsymbol{X}}^{n+1}_r)^l(x)| \leq C, \quad |(\widetilde{\boldsymbol{X}}^{n+1}_L)^l(x)| \leq C\theta_1^l\exp(-q\theta_1 x), \quad |(\widetilde{\boldsymbol{X}}^{n+1}_R)^l(x)| \leq C\theta_2^l\exp(-q\theta_2(1-x)), \quad 0 \leq l \leq p,$$

where θ_1 and θ_2 have the same values as those given in Lemma 2.5. With $0 \leq l \leq p$, the derivative bounds are as follows, specifically for a specified p and a fixed integer $0 < q < 1$.

$$\left|\frac{d^l\widetilde{\boldsymbol{X}}^{n+1}(x)}{dx^l}\right| \leq C(1 + \theta_1^l\exp(-q\theta_1 x) + \theta_2^l\exp(-q\theta_2(1-x))).$$

Proof. The proof follows the ideas and techniques used in [25], where an elliptic scalar singularly perturbed problem with two parameter was considered. □

3.2. Shishkin mesh generation

It takes a lot of computing power and a lot of nodal points to achieve uniform convergence on a uniform mesh in spatial variable. Therefore, it is crucial to construct numerical schemes that are accurate and unaffected by the value of the perturbation parameters. The fitted mesh technique, which uses a specialized layer-adapted mesh, successfully addresses these issues. In order to get a dense distribution of points in the layer region, we use a piecewise uniform mesh of Shishkin type for the spatial discretization. To construct this mesh, first we define the transition parameters ξ_1 and ξ_2, which divide the domain into inner and outer areas. Taking into account

Table 1
Values of $\mathcal{B}_m$, $\mathcal{B}'_m$, and $\mathcal{B}''_m$ at nodal points.

	$j = m-1$	$j = m$	$j = m+1$	Otherwise
$\mathcal{B}_m(x_j)$	$\frac{1}{6}$	$\frac{2}{3}$	$\frac{1}{6}$	0
$\mathcal{B}'_m(x_j)$	$-\frac{1}{2\widetilde{h}_m}$	0	$\frac{1}{2\widetilde{h}_m}$	0
$\mathcal{B}''_m(x_j)$	$\frac{1}{\widetilde{h}_m^2}$	$-\frac{2}{\widetilde{h}_m^2}$	$\frac{1}{\widetilde{h}_m^2}$	0

the behavior of the exact solution proven previously, the transition parameters are given by

$$\xi_1 = \begin{cases} \min\left\{\frac{1}{4}, \frac{4\sqrt{\nu_1}}{\sqrt{\eta\alpha}} \ln \mathcal{N}_x\right\}, & \text{if } \alpha\nu_2^2 \le \eta\nu_1, \\ \min\left\{\frac{1}{4}, \frac{4\nu_1}{\nu_2\alpha} \ln \mathcal{N}_x\right\}, & \text{if } \alpha\nu_2^2 > \eta\nu_1, \end{cases} \qquad \xi_2 = \begin{cases} \min\left\{\frac{1}{4}, \frac{4\sqrt{\nu_1}}{\sqrt{\eta\alpha}} \ln \mathcal{N}_x\right\}, & \text{if } \alpha\nu_2^2 \le \eta\nu_1, \\ \min\left\{\frac{1}{4}, \frac{4\nu_2}{\eta} \ln \mathcal{N}_x\right\}, & \text{if } \alpha\nu_2^2 > \eta\nu_1. \end{cases}$$

Using these transition parameters, the interval $[0,1]$ is partitioned into three subregions: $[0,\zeta_1]$, $[\zeta_1, 1-\zeta_2]$ and $[1-\zeta_2, 1]$. We allocate $\mathcal{N}_x/4$ points within the subintervals $[0,\zeta_1]$ and $[1-\zeta_2, 1]$, while assigning $\mathcal{N}_x/2$ points to $[\zeta_1, 1-\zeta_2]$. The spatial mesh is represented as $\Lambda^{\mathcal{N}_x} = \{x_m\}_{m=0}^{\mathcal{N}_x}$, with the interval length given by $\widetilde{h}_m = s_m - s_{m-1},\ m = 1, 2, \dots, \mathcal{N}_x$, corresponding to the subinterval $I_m = (s_{m-1}, s_m)$.

$$\widetilde{h}_m = \begin{cases} \frac{4\xi_1}{\mathcal{N}_x}, & m = 1, 2, \dots, \frac{\mathcal{N}_x}{4}, \\ \frac{2(1-\xi_1-\xi_2)}{\mathcal{N}_x}, & m = \frac{\mathcal{N}_x}{4}+1, \dots, \frac{3\mathcal{N}_x}{4}, \\ \frac{4\xi_2}{\mathcal{N}_x}, & m = \frac{3\mathcal{N}_x}{4}+1, \dots, \mathcal{N}_x, \end{cases} \qquad x_m = \begin{cases} m\widetilde{h}_m, & m = 1, 2, \dots, \frac{\mathcal{N}_x}{4}, \\ \xi_1 + (m - \frac{\mathcal{N}_x}{4})\widetilde{h}_m, & m = \frac{\mathcal{N}_x}{4}+1, \dots, \frac{3\mathcal{N}_x}{4}, \\ 1-\xi_2 + (m - \frac{3\mathcal{N}_x}{4})\widetilde{h}_m, & m = \frac{3\mathcal{N}_x}{4}+1, \dots, \mathcal{N}_x, \end{cases}$$

with $x_0 = 0$.

3.3. Spatial discretization

$\mathcal{B}$-splines are used for the spatial discretization in order to build an accurate and effective numerical scheme. To ensure continuity at the domain boundaries, four fictitious nodes, x_{-2}, x_{-1}, $x_{\mathcal{N}_x+1}$, and $x_{\mathcal{N}_x+2}$, are introduced. The nodes x_{-2} and x_{-1} are placed on the left side of $\Lambda^{\mathcal{N}_x}$, while $x_{\mathcal{N}_x+1}$ and $x_{\mathcal{N}_x+2}$ are positioned on the right side.

For the definition and fundamental characteristics of $\mathcal{B}$-splines, see [26]. They are given by

$$\mathcal{B}_m(x) = \frac{\Delta^4 \Xi_x(x_{m-1})}{\widehat{h}_m^3},$$

where

$$\Xi_x(x_{m-1}) = (x_{m-1} - x)_+^3 = \begin{cases} (x_{m-1} - x)^3, & x \le x_{m-1}, \\ 0, & x \ge x_{m-1}. \end{cases}$$

For $m = -1, \dots, \mathcal{N}_x + 1$, the functions $\mathcal{B}_m$ are provided by

$$\mathcal{B}_m(x) = \frac{1}{\widehat{h}_m^3} \begin{cases} (x - x_{m-2})^3, & x_{m-2} \le x \le x_{m-1}, \\ \widetilde{h}_m^3 + 3\widetilde{h}_m^2(x - x_{m-1}) + 3\widetilde{h}_m(x - x_{m-1})^2 - 3(x - x_{m-1})^3, & x_{m-1} \le x \le x_m, \\ \widetilde{h}_m^3 + 3\widetilde{h}_m^2(x_{m+1} - x) + 3\widetilde{h}_m(x_{m+1} - x)^2 - 3(x_{m+1} - x)^3, & x_m \le x \le x_{m+1}, \\ (x_{m+2} - x)^3, & x_{m+1} \le x \le x_{m+2}, \\ 0, & \text{otherwise.} \end{cases}$$

Readers interested in certain fundamental characteristics of $\mathcal{B}$-splines are advised to consult the Ref. [27]. Those qualities make it simple to obtain the Table 1.

We may use a linear combination of the $\mathcal{B}$-spline basis functions to obtain an approximate solution at time s_{n+1}, i.e., we consider

$$\mathcal{X}_k^{n+1}(x) = \sum_{m=-1}^{\mathcal{N}_x+1} w_{m;k}^{n+1} \mathcal{B}_m(x).$$

The unknown coefficients $w_{m;k}^{n+1}$ to be found at each time step using a variant of the Thomas approach. A system of linear equations for the unknown coefficients is produced by substituting the B-spline representation into the discretized version of the governing

equations (Eq. (3.3)). Then, we have

$$\begin{aligned}
\mathcal{L}_1\boldsymbol{\mathcal{X}}^{n+1} \equiv & -\frac{\nu_1}{2}\left(\frac{1}{\widetilde{h}_m^2}w_{m-1;1}^{n+1}-\frac{2}{\widetilde{h}_m^2}w_{m;1}^{n+1}+\frac{1}{\widetilde{h}_m^2}w_{m+1;1}^{n+1}\right)-\nu_2\frac{p_{11}^{n+\frac{1}{2}}(x_m)}{2}\left(-\frac{1}{2\widetilde{h}_m}w_{m-1;1}^{n+1}+\frac{1}{2\widetilde{h}_m}w_{m+1;1}^{n+1}\right)\\
&+\left(\frac{1}{\Delta s}+\frac{q_{11}^{n+\frac{1}{2}}(x_m)}{2}\right)\left(\frac{1}{6}w_{m-1;1}^{n+1}+\frac{2}{3}w_{m;1}^{n+1}+\frac{1}{6}w_{m+1;1}^{n+1}\right)\\
&+\frac{q_{12}^{n+\frac{1}{2}}(x_m)}{2}\left(\frac{1}{6}w_{m-1;2}^{n+1}+\frac{2}{3}w_{m;2}^{n+1}+\frac{1}{6}w_{m+1;2}^{n+1}\right)\\
&=g_1^{n+\frac{1}{2}}(x_m)+\frac{\nu_1}{2}\left(\frac{1}{\widetilde{h}_m^2}w_{m-1;1}^{n}-\frac{2}{\widetilde{h}_m^2}w_{m;1}^{n}+\frac{1}{\widetilde{h}_m^2}w_{m+1;1}^{n}\right)\\
&+\nu_2\frac{p_{11}^{n+\frac{1}{2}}(x_m)}{2}\left(-\frac{1}{2\widetilde{h}_m}w_{m-1;1}^{n}+\frac{1}{2\widetilde{h}_m}w_{m+1;1}^{n}\right)\\
&+\left(\frac{1}{\Delta s}-\frac{q_{11}^{n+\frac{1}{2}}(x_m)}{2}\right)\left(\frac{1}{6}w_{m-1;1}^{n}+\frac{2}{3}w_{m;1}^{n}+\frac{1}{6}w_{m+1;1}^{n}\right)\\
&-\frac{q_{12}^{n+\frac{1}{2}}(x_m)}{2}\left(\frac{1}{6}w_{m-1;2}^{n}+\frac{2}{3}w_{m;2}^{n}+\frac{1}{6}w_{m+1;2}^{n}\right),\ 0\le m\le\mathcal{N}_x,\ 0\le n\le\mathcal{N}_s-1,
\end{aligned}\tag{3.6a}$$

$$\begin{aligned}
\mathcal{L}_2\boldsymbol{\mathcal{X}}^{n+1} \equiv & -\frac{\nu_1}{2}\left(\frac{1}{\widetilde{h}_m^2}w_{m-1;2}^{n+1}-\frac{2}{\widetilde{h}_m^2}w_{m;2}^{n+1}+\frac{1}{\widetilde{h}_m^2}w_{m+1;2}^{n+1}\right)-\nu_2\frac{p_{22}^{n+\frac{1}{2}}(x_m)}{2}\left(-\frac{1}{2\widetilde{h}_m}w_{m-1;2}^{n+1}+\frac{1}{2\widetilde{h}_m}w_{m+1;2}^{n+1}\right)\\
&+\left(\frac{1}{\Delta s}+\frac{q_{22}^{n+\frac{1}{2}}(x_m)}{2}\right)\left(\frac{1}{6}w_{m-1;2}^{n+1}+\frac{2}{3}w_{m;2}^{n+1}+\frac{1}{6}w_{m+1;2}^{n+1}\right)\\
&+\frac{q_{21}^{n+\frac{1}{2}}(x_m)}{2}\left(\frac{1}{6}w_{m-1;1}^{n+1}+\frac{2}{3}w_{m;1}^{n+1}+\frac{1}{6}w_{m+1;1}^{n+1}\right)\\
&=g_2^{n+\frac{1}{2}}(x_m)+\frac{\nu_1}{2}\left(\frac{1}{\widetilde{h}_m^2}w_{m-1;2}^{n}-\frac{2}{\widetilde{h}_m^2}w_{m;2}^{n}+\frac{1}{\widetilde{h}_m^2}w_{m+1;2}^{n}\right)\\
&+\nu_2\frac{p_{22}^{n+\frac{1}{2}}(x_m)}{2}\left(-\frac{1}{2\widetilde{h}_m}w_{m-1;2}^{n}+\frac{1}{2\widetilde{h}_m}w_{m+1;2}^{n}\right)\\
&+\left(\frac{1}{\Delta s}-\frac{q_{22}^{n+\frac{1}{2}}(x_m)}{2}\right)\left(\frac{1}{6}w_{m-1;2}^{n}+\frac{2}{3}w_{m;2}^{n}+\frac{1}{6}w_{m+1;2}^{n}\right)\\
&-\frac{q_{21}^{n+\frac{1}{2}}(x_m)}{2}\left(\frac{1}{6}w_{m-1;1}^{n}+\frac{2}{3}w_{m;1}^{n}+\frac{1}{6}w_{m+1;1}^{n}\right),\ 0\le m\le\mathcal{N}_x,\ 0\le n\le\mathcal{N}_s-1,
\end{aligned}\tag{3.6b}$$

with boundary conditions given by

$$\frac{1}{6}w_{-1;1}^{n+1}+\frac{2}{3}w_{0;1}^{n+1}+\frac{1}{6}w_{1;1}^{n+1}=\mathfrak{l}_1(s_{n+1}),\tag{3.6c}$$

$$\frac{1}{6}w_{\mathcal{N}_x-1;1}^{n+1}+\frac{2}{3}w_{\mathcal{N}_x;1}^{n+1}+\frac{1}{6}w_{\mathcal{N}_x+1;1}^{n+1}=\mathfrak{m}_1(s_{n+1}),\ 0\le n\le\mathcal{N}_s-1,\tag{3.6d}$$

$$\frac{1}{6}w_{-1;2}^{n+1}+\frac{2}{3}w_{0;2}^{n+1}+\frac{1}{6}w_{1;2}^{n+1}=\mathfrak{l}_2(s_{n+1}),\tag{3.6e}$$

$$\frac{1}{6}w_{\mathcal{N}_x-1;2}^{n+1}+\frac{2}{3}w_{\mathcal{N}_x;2}^{n+1}+\frac{1}{6}w_{\mathcal{N}_x+1;2}^{n+1}=\mathfrak{m}_2(s_{n+1}),\ 0\le n\le\mathcal{N}_s-1.\tag{3.6f}$$

Eqs. (3.6a) and (3.6b) provide the following results once the terms are collected:

$$\begin{aligned}
\mathcal{L}_1\boldsymbol{\mathcal{X}}^{n+1} \equiv & \ w_{m-1;1}^{n+1}\left[\frac{-\nu_1}{2\widetilde{h}_m^2}+\nu_2\frac{p_{11}^{n+\frac{1}{2}}(x_m)}{4\widetilde{h}_m}+\frac{1}{6}\left(\frac{1}{\Delta s}+\frac{q_{11}^{n+\frac{1}{2}}(x_m)}{2}\right)\right]+w_{m;1}^{n+1}\left[\frac{\nu_1}{\widetilde{h}_m^2}+\frac{2}{3}\left(\frac{1}{\Delta s}+\frac{q_{11}^{n+\frac{1}{2}}(x_m)}{2}\right)\right]\\
&+w_{m+1;1}^{n+1}\left[\frac{-\nu_1}{2\widetilde{h}_m^2}-\nu_2\frac{p_{11}^{n+\frac{1}{2}}(x_m)}{4\widetilde{h}_m}+\frac{1}{6}\left(\frac{1}{\Delta s}+\frac{q_{11}^{n+\frac{1}{2}}(x_m)}{2}\right)\right]+w_{m-1;2}^{n+1}\left(\frac{q_{12}^{n+\frac{1}{2}}(x_m)}{12}\right)\\
&+w_{m;2}^{n+1}\left(\frac{q_{12}^{n+\frac{1}{2}}(x_m)}{3}\right)+w_{m+1;2}^{n+1}\left(\frac{q_{12}^{n+\frac{1}{2}}(x_m)}{12}\right)=g_1^{n+\frac{1}{2}}(x_m)+w_{m-1;1}^{n}\left[\frac{\nu_1}{2\widetilde{h}_m^2}-\nu_2\frac{p_{11}^{n+\frac{1}{2}}(x_m)}{4\widetilde{h}_m}\right.
\end{aligned}$$

$$+\frac{1}{6}\left(\frac{1}{\Delta s}-\frac{q_{11}^{n+\frac{1}{2}}(x_m)}{2}\right)\Bigg]+w_{m;1}^{n}\left[-\frac{\nu_1}{\widetilde{h}_m^2}+\frac{2}{3}\left(\frac{1}{\Delta s}-\frac{q_{11}^{n+\frac{1}{2}}(x_m)}{2}\right)\right]+w_{m+1;1}^{n}\left[\frac{\nu_1}{2\widetilde{h}_m^2}+\nu_2\frac{p_{11}^{n+\frac{1}{2}}(x_m)}{4\widetilde{h}_m}\right.$$
$$\left.+\frac{1}{6}\left(\frac{1}{\Delta s}-\frac{q_{11}^{n+\frac{1}{2}}(x_m)}{2}\right)\right]-w_{m-1;2}^{n}\left(\frac{q_{12}^{n+\frac{1}{2}}(x_m)}{12}\right)-w_{m;2}^{n}\left(\frac{q_{12}^{n+\frac{1}{2}}(x_m)}{3}\right)-w_{m+1;2}^{n}\left(\frac{q_{12}^{n+\frac{1}{2}}(x_m)}{12}\right), \tag{3.7a}$$

$$\mathcal{L}_2\mathcal{X}^{n+1}\equiv w_{m-1;1}^{n+1}\left(\frac{q_{21}^{n+\frac{1}{2}}(x_m)}{12}\right)+w_{m;1}^{n+1}\left(\frac{q_{21}^{n+\frac{1}{2}}(x_m)}{3}\right)+w_{m+1;1}^{n+1}\left(\frac{q_{21}^{n+\frac{1}{2}}(x_m)}{12}\right)+w_{m-1;2}^{n+1}\left[\frac{-\nu_1}{2\widetilde{h}_m^2}+\nu_2\frac{p_{22}^{n+\frac{1}{2}}(x_m)}{4\widetilde{h}_m}\right.$$
$$+\frac{1}{6}\left(\frac{1}{\Delta s}+\frac{q_{22}^{n+\frac{1}{2}}(x_m)}{2}\right)\Bigg]+w_{m;2}^{n+1}\left[\frac{\nu_1}{\widetilde{h}_m^2}+\frac{2}{3}\left(\frac{1}{\Delta s}+\frac{q_{22}^{n+\frac{1}{2}}(x_m)}{2}\right)\right]+w_{m+1;2}^{n+1}\left[\frac{-\nu_1}{2\widetilde{h}_m^2}-\nu_2\frac{p_{22}^{n+\frac{1}{2}}(x_m)}{4\widetilde{h}_m}\right.$$
$$\left.+\frac{1}{6}\left(\frac{1}{\Delta s}+\frac{q_{22}^{n+\frac{1}{2}}(x_m)}{2}\right)\right]=g_2^{n+\frac{1}{2}}(x_m)-w_{m-1;1}^{n}\left(\frac{q_{21}^{n+\frac{1}{2}}(x_m)}{12}\right)-w_{m;1}^{n}\left(\frac{q_{21}^{n+\frac{1}{2}}(x_m)}{3}\right)$$
$$-w_{m+1;1}^{n}\left(\frac{q_{21}^{n+\frac{1}{2}}(x_m)}{12}\right)+w_{m-1;2}^{n}\left[\frac{\nu_1}{2\widetilde{h}_m^2}-\nu_2\frac{p_{22}^{n+\frac{1}{2}}(x_m)}{4\widetilde{h}_m}+\frac{1}{6}\left(\frac{1}{\Delta s}-\frac{q_{22}^{n+\frac{1}{2}}(x_m)}{2}\right)\right]+w_{m;2}^{n}\left[-\frac{\nu_1}{\widetilde{h}_m^2}\right.$$
$$\left.+\frac{2}{3}\left(\frac{1}{\Delta s}-\frac{q_{22}^{n+\frac{1}{2}}(x_m)}{2}\right)\right]+w_{m+1;2}^{n}\left[\frac{\nu_1}{2\widetilde{h}_m^2}+\nu_2\frac{p_{22}^{n+\frac{1}{2}}(x_m)}{4\widetilde{h}_m}+\frac{1}{6}\left(\frac{1}{\Delta s}-\frac{q_{22}^{n+\frac{1}{2}}(x_m)}{2}\right)\right]. \tag{3.7b}$$

With the Eqs. (3.6c)–(3.6f), (3.7a), and (3.7b) taken into account, we obtain the following linear system

$$\mathcal{A}\boldsymbol{w}^{n+1}=\mathcal{B}, \tag{3.8}$$

where $\mathcal{B}=C\boldsymbol{w}^{n}+D$ and the corresponding matrices are defined by

$$\mathcal{A}=\begin{bmatrix}\mathcal{A}_1 & \mathcal{A}_2\\ \mathcal{A}_3 & \mathcal{A}_4\end{bmatrix},\quad C=\begin{bmatrix}C_1 & C_2\\ C_3 & C_4\end{bmatrix},$$
$$\boldsymbol{w}^{n+1}=\Big(\underbrace{w_{-1,1}^{n+1},w_{0,1}^{n+1},\ldots,w_{\mathcal{N}_x,1}^{n+1},w_{\mathcal{N}_x+1,1}^{n+1}}_{1^{st}\text{ component}},\underbrace{w_{-1,2}^{n+1},w_{0,2}^{n+1},\ldots,w_{\mathcal{N}_x,2}^{n+1},w_{\mathcal{N}_x+1,2}^{n+1}}_{2^{nd}\text{ component}}\Big)^{T},$$

with

$$\mathcal{A}_1=[1/6,2/3,1/6,0,\ldots,0;\text{tridiag}(\mathrm{p}_1(x_m),\mathrm{p}_2(x_m),\mathrm{p}_3(x_m));0,\ldots,0,1/6,2/3,1/6],$$
$$\mathcal{A}_2=[0,0,\ldots,0;\text{tridiag}(\mathrm{q}_1(x_m),\mathrm{q}_2(x_m),\mathrm{q}_1(x_m));0,\ldots,0,0],$$
$$\mathcal{A}_3=[0,0,\ldots,0;\text{tridiag}(\mathrm{r}_1(x_m),\mathrm{r}_2(x_m),\mathrm{r}_1(x_m));0,\ldots,0,0],$$
$$\mathcal{A}_4=[1/6,2/3,1/6,0,\ldots,0;\text{tridiag}(\mathrm{s}_1(x_m),\mathrm{s}_2(x_m),\mathrm{s}_3(x_m));0,\ldots,0,1/6,2/3,1/6],$$
$$C_1=[0,0,\ldots,0;\text{tridiag}(\mathrm{t}_1(x_m),\mathrm{t}_2(x_m),\mathrm{t}_3(x_m));0,\ldots,0,0],$$
$$C_2=[0,0,\ldots,0;\text{tridiag}(\mathrm{u}_1(x_m),\mathrm{u}_2(x_m),\mathrm{u}_1(x_m));0,\ldots,0,0],$$
$$C_3=[0,0,\ldots,0;\text{tridiag}(\mathrm{v}_1(x_m),\mathrm{v}_2(x_m),\mathrm{v}_1(x_m));0,\ldots,0,0],$$
$$C_4=[0,0,\ldots,0;\text{tridiag}(\mathrm{w}_1(x_m),\mathrm{w}_2(x_m),\mathrm{w}_3(x_m));0,\ldots,0,0].$$

Since $\mathcal{A}$ has a block tridiagonal structure, we analyze its diagonal dominance and also its condition number.

The matrix norm is given by

$$\|\mathcal{A}^{-1}\|_\infty=\max_{1\le m\le\mathcal{N}_x}\sum_{n=1}^{\mathcal{N}_s}|(\mathcal{A}^{-1})_{mn}|.$$

The condition number of the matrix $\mathcal{A}$ in the infinity norm is given by

$$\kappa_\infty(\mathcal{A})=\|\mathcal{A}\|_\infty\|\mathcal{A}^{-1}\|_\infty.$$

The Block Thomas Algorithm guarantees an efficient inversion process for the tridiagonal matrices under consideration. However, the existence of stiffness perturbation parameters may cause $\|\mathcal{A}^{-1}\|_\infty$ to grow, which would raise the condition number $\kappa_\infty(\mathcal{A})$. Because of the potential for numerical instability caused by this rise in the condition number, it is not practicable to compute $\mathcal{A}^{-1}$ explicitly. Instead of solving $\mathcal{A}^{-1}$ directly, the problem is addressed repeatedly in MATLAB to improve numerical stability rather than explicitly computing A^{-1}.

These matrices, which have the arguments provided, are tridiagonal and of order $(\mathcal{N}_x+3)\times(\mathcal{N}_x+3)$. The corresponding elements of these matrices for $m=0,1,\ldots,\mathcal{N}_x$ are provided by

$$\mathrm{p}_1(x_m)=-\frac{\nu_1}{2\widetilde{h}_m^2}+\nu_2\frac{p_{11}^{n+\frac{1}{2}}(x_m)}{4\widetilde{h}_m}+\frac{1}{6}\left(\frac{1}{\Delta s}+\frac{q_{11}^{n+\frac{1}{2}}(x_m)}{2}\right),\ \mathrm{p}_2(x_m)=\frac{\nu_1}{\widetilde{h}_m^2}+\frac{2}{3}\left(\frac{1}{\Delta s}+\frac{q_{11}^{n+\frac{1}{2}}(x_m)}{2}\right),$$

$$\mathrm{p}_3(x_m) = -\frac{\nu_1}{2\widetilde{h}_m^2} - \nu_2\frac{p_{11}^{n+\frac{1}{2}}(x_m)}{4\widetilde{h}_m} + \frac{1}{6}\left(\frac{1}{\Delta s} + \frac{q_{11}^{n+\frac{1}{2}}(x_m)}{2}\right),\ \mathrm{q}_1(x_m) = \frac{q_{12}^{n+\frac{1}{2}}(x_m)}{12},$$

$$\mathrm{q}_2(x_m) = \frac{q_{12}^{n+\frac{1}{2}}(x_m)}{3},\ \mathrm{r}_1(x_m) = \frac{q_{21}^{n+\frac{1}{2}}(x_m)}{12},\ \mathrm{r}_2(x_m) = \frac{q_{21}^{n+\frac{1}{2}}(x_m)}{3},$$

$$\mathrm{s}_1(x_m) = -\frac{\nu_1}{2\widetilde{h}_m^2} + \nu_2\frac{p_{22}^{n+\frac{1}{2}}(x_m)}{4\widetilde{h}_m} + \frac{1}{6}\left(\frac{1}{\Delta s} + \frac{q_{22}^{n+\frac{1}{2}}(x_m)}{2}\right),\ \mathrm{s}_2(x_m) = \frac{\nu_1}{\widetilde{h}_m^2} + \frac{2}{3}\left(\frac{1}{\Delta s} + \frac{q_{22}^{n+\frac{1}{2}}(x_m)}{2}\right),$$

$$\mathrm{s}_3(x_m) = -\frac{\nu_1}{2\widetilde{h}_m^2} - \nu_2\frac{p_{22}^{n+\frac{1}{2}}(x_m)}{4\widetilde{h}_m} + \frac{1}{6}\left(\frac{1}{\Delta s} + \frac{q_{22}^{n+\frac{1}{2}}(x_m)}{2}\right),$$

$$\mathrm{t}_1(x_m) = \frac{\nu_1}{2\widetilde{h}_m^2} - \nu_2\frac{p_{11}^{n+\frac{1}{2}}(x_m)}{4\widetilde{h}_m} + \frac{1}{6}\left(\frac{1}{\Delta s} - \frac{q_{11}^{n+\frac{1}{2}}(x_m)}{2}\right),\ \mathrm{t}_2(x_m) = -\frac{\nu_1}{\widetilde{h}_m^2} + \frac{2}{3}\left(\frac{1}{\Delta s} - \frac{q_{11}^{n+\frac{1}{2}}(x_m)}{2}\right),$$

$$\mathrm{t}_3(x_m) = \frac{\nu_1}{2\widetilde{h}_m^2} + \nu_2\frac{p_{11}^{n+\frac{1}{2}}(x_m)}{4\widetilde{h}_m} + \frac{1}{6}\left(\frac{1}{\Delta s} - \frac{q_{11}^{n+\frac{1}{2}}(x_m)}{2}\right),\ \mathrm{u}_1(x_m) = -\frac{q_{12}^{n+\frac{1}{2}}(x_m)}{12},$$

$$\mathrm{u}_2(x_m) = -\frac{q_{12}^{n+\frac{1}{2}}(x_m)}{3},\ \mathrm{v}_1(x_m) = -\frac{q_{21}^{n+\frac{1}{2}}(x_m)}{12},\ \mathrm{v}_2(x_m) = -\frac{q_{21}^{n+\frac{1}{2}}(x_m)}{3},$$

$$\mathrm{w}_1(x_m) = \frac{\nu_1}{2\widetilde{h}_m^2} - \nu_2\frac{p_{22}^{n+\frac{1}{2}}(x_m)}{4\widetilde{h}_m} + \frac{1}{6}\left(\frac{1}{\Delta s} - \frac{q_{22}^{n+\frac{1}{2}}(x_m)}{2}\right),\ \mathrm{w}_2(x_m) = -\frac{\nu_1}{\widetilde{h}_m^2} + \frac{2}{3}\left(\frac{1}{\Delta s} - \frac{q_{22}^{n+\frac{1}{2}}(x_m)}{2}\right),$$

$$\mathrm{w}_3(x_m) = \frac{\nu_1}{2\widetilde{h}_m^2} + \nu_2\frac{p_{22}^{n+\frac{1}{2}}(x_m)}{4\widetilde{h}_m} + \frac{1}{6}\left(\frac{1}{\Delta s} - \frac{q_{22}^{n+\frac{1}{2}}(x_m)}{2}\right),$$

$$\mathcal{D} = \left(\mathfrak{l}_1(s_{n+1}), g_1^{n+\frac{1}{2}}(x_0), \ldots, g_1^{n+\frac{1}{2}}(x_{\mathcal{N}_x}), \mathfrak{m}_1(s_{n+1}), \mathfrak{l}_2(s_{n+1}), g_2^{n+\frac{1}{2}}(x_0), \ldots, g_2^{n+\frac{1}{2}}(x_{\mathcal{N}_x}), \mathfrak{m}_2(s_{n+1})\right)^T.$$

4. Uniform convergence

Lemma 4.1. *For cubic B-spline functions, the following inequality is valid.*

$$\sum_{n=-1}^{\mathcal{N}_x+1} |\mathcal{B}_n(x)| \le 10, \quad x \in [0,1].$$

Proof. We follows the methodology described in [24]. Then, for a nodal point x_l, we have

$$\mathcal{B}_{l-1}(x_l) = 1,\ \mathcal{B}_l(x_l) = 4,\ \mathcal{B}_{l+1}(x_l) = 1.$$

So, it follows

$$\sum_{n=-1}^{\mathcal{N}_x+1} |\mathcal{B}_l(x_l)| = |\mathcal{B}_{l-1}(x_l)| + |\mathcal{B}_l(x_l)| + |\mathcal{B}_{l+1}(x_l)| = 1 + 4 + 1 = 6.$$

For $x \in [x_{l-1}, x_l]$, we obtain

$$\sum_{n=-1}^{\mathcal{N}_x+1} |\mathcal{B}_n(x)| = |\mathcal{B}_{l-2}(x)| + |\mathcal{B}_{l-1}(x)| + |\mathcal{B}_l(x)| + |\mathcal{B}_{l+1}(x)| \le 1 + 4 + 4 + 1 = 10.$$

Thus, $\sum_{n=-1}^{\mathcal{N}_x+1} |\mathcal{B}_n(x)| \le 10$, $\forall\, x \in [0,1]$, which is the required result. □

Next result proves the uniform convergence of the spatial discretization.

Theorem 4.2. *If $g \in C^2[0,1]$, then the approximated solution $\boldsymbol{\mathcal{X}}^{n+1}(x)$ to the solution $\widetilde{\mathbf{X}}(x)$ of (3.1) on $\Omega_s^{\mathcal{N}_s}$ at the $(n+1)$th time level satisfies*

$$\sup_{0<\nu_1,\nu_2\le 1} \|\boldsymbol{\mathcal{X}}^{n+1} - \widetilde{\mathbf{X}}^{n+1}\| \le C\mathcal{N}_x^{-2}(\ln \mathcal{N}_x)^2.$$

Proof. To solve the problem (3.4), the special spline interpolant $\mathbf{X}_{\mathcal{N}_x}(x)$ is provided by

$$\boldsymbol{X}_{\mathcal{N}_x}(x) = \sum_{m=-1}^{\mathcal{N}_x+1} w_{m;l}^{n+1}\mathcal{B}_m(x).$$

For simplicity, we denote $\widetilde{\mathbf{X}}$ by $\widetilde{\mathbf{X}}^{n+1}$. Following to [28], we can obtain

$$\|D^j(\widetilde{\mathbf{X}} - \mathbf{X}_{\mathcal{N}_x})(x_m)\|_\infty \le \psi_j \|\widetilde{\mathbf{X}}^{(4)}\| \overline{h}^{4-j}, \quad j = 0, 1, 2, \tag{4.1}$$

where D denotes the derivative, $\overline{h} = \max_m \widetilde{h}_m$ and ψ_j are constants. The estimations (4.1) and use of Lemma 3.3 clearly shows that

$$\begin{aligned}
|\mathcal{L}_1\widetilde{\mathbf{X}}(x) - \mathcal{L}_1\mathbf{X}_{\mathcal{N}_x}| &\le \left(-\frac{\nu_1}{2}\psi_2\overline{h}^2 - \frac{\nu_2}{2}\left\|p_{11}^{n+1/2}\right\|\psi_1\overline{h}^3 + \frac{1}{2}\left\|\mathfrak{R}_1^{n+1/2}\right\|\psi_0\overline{h}^4\right)|\widetilde{\mathbf{X}}^{(4)}(x)| \\
&\le C\left(-\nu_1\psi_2\overline{h}^2 - \nu_2\left\|p_{11}^{n+1/2}\right\|\psi_1\overline{h}^3 + \left\|\mathfrak{R}_1^{n+1/2}\right\|\psi_0\overline{h}^4\right)[1 + \theta_1^4\exp(-q\theta_1 x) \\
&\quad + \theta_2^4\exp(-q\theta_2(1-x))], \qquad (4.2) \\
|\mathcal{L}_2\widetilde{\mathbf{X}}(x) - \mathcal{L}_2\mathbf{X}_{\mathcal{N}_x}| &\le \left(-\frac{\nu_1}{2}\psi_2\overline{h}^2 - \frac{\nu_2}{2}\left\|p_{22}^{n+1/2}\right\|\psi_1\overline{h}^3 + \frac{1}{2}\left\|\mathfrak{R}_2^{n+1/2}\right\|\psi_0\overline{h}^4\right)|\widetilde{\mathbf{X}}^{(4)}(x)| \\
&\le C\left(-\nu_1\psi_2\overline{h}^2 - \nu_2\left\|p_{22}^{n+1/2}\right\|\psi_1\overline{h}^3 + \left\|\mathfrak{R}_2^{n+1/2}\right\|\psi_0\overline{h}^4\right)[1 + \theta_1^4\exp(-q\theta_1 x) \\
&\quad + \theta_2^4\exp(-q\theta_2(1-x))], \qquad (4.3)
\end{aligned}$$

where

$$\mathfrak{R}_k^{m+\frac{1}{2}}(x) = \frac{1}{\Delta s} + \frac{q_{kk}^{m+\frac{1}{2}}(x)}{2}.$$

The bounds for the three distinct intervals $[0, \xi_1], [\xi_1, 1-\xi_2]$ and $[1-\xi_2, 1]$ are established independently.

First, we consider the case when $\alpha\nu_2^2 \le \eta\nu_1$ holds.

Then, if $x_m \in [0, \xi_1]$, i.e., $1 \le m \le \dfrac{\mathcal{N}_x}{4}$, it holds $\exp(-\theta_1 x_m) \le 1$ and $\exp(-\theta_2(1-x_m)) \le \exp(-\theta_1(1-\xi_1)) \le \mathcal{N}_x^q$. Thus, (4.2) and (4.3) yield

$$|\mathcal{L}_1\widetilde{\mathbf{X}}(x_m) - \mathcal{L}_1\mathbf{X}_{\mathcal{N}_x}| \le C\left(\nu_1\psi_2\overline{h}^2 + \nu_2\left\|p_{11}^{n+1/2}\right\|\psi_1\overline{h}^3 + \left\|\mathfrak{R}_1^{n+1/2}\right\|\psi_0\overline{h}^4\right)(1 + \theta_1^4 + \theta_2^4), \tag{4.4}$$

and

$$|\mathcal{L}_2\widetilde{\mathbf{X}}(x_m) - \mathcal{L}_2\mathbf{X}_{\mathcal{N}_x}| \le C\left(\nu_1\psi_2\overline{h}^2 + \nu_2\left\|p_{22}^{n+1/2}\right\|\psi_1\overline{h}^3 + \left\|\mathfrak{R}_2^{n+1/2}\right\|\psi_0\overline{h}^4\right)(1 + \theta_1^4 + \theta_2^4). \tag{4.5}$$

Also, $\overline{h} = \dfrac{4\xi_1}{\mathcal{N}_x} = \dfrac{16\sqrt{\nu_1}}{\mathcal{N}_x\sqrt{\eta\alpha}}\ln\mathcal{N}_x$, therefore, we have

$$\begin{aligned}
\nu_1\psi_2\overline{h}^2 &= \nu_1\psi_2\left(\frac{16\sqrt{\nu_1}}{\mathcal{N}_x\sqrt{\eta\alpha}}\ln\mathcal{N}_x\right)^2 \le C\mathcal{N}_x^{-2}(\ln\mathcal{N}_x)^2, \\
\nu_2\left\|p_{kk}^{n+1/2}\right\|\psi_1\overline{h}^3 &= \nu_2\left\|p_{kk}^{n+1/2}\right\|\psi_1\left(\frac{16\sqrt{\nu_1}}{\mathcal{N}_x\sqrt{\eta\alpha}}\ln\mathcal{N}_x\right)^3 \le C\mathcal{N}_x^{-3}(\ln\mathcal{N}_x)^3, \quad k = 1, 2, \\
\left\|\mathfrak{R}_k^{n+1/2}\right\|\psi_0\overline{h}^4 &\le C\mathcal{N}_x^{-4}(\ln\mathcal{N}_x)^4, \quad k = 1, 2, \\
\nu_1\psi_2\overline{h}^2\theta_1^4 &= \nu_1\psi_2\left(\frac{16\sqrt{\nu_1}}{\mathcal{N}_x\sqrt{\eta\alpha}}\ln\mathcal{N}_x\right)^2\left(\frac{\sqrt{\eta\alpha}}{\sqrt{\nu_1}}\right)^4 \le C\mathcal{N}_x^{-2}(\ln\mathcal{N}_x)^2, \\
\nu_2\left\|p_{kk}^{n+1/2}\right\|\psi_1\overline{h}^3\theta_1^4 &= \nu_2\left\|p_{kk}^{n+1/2}\right\|\psi_1\left(\frac{16\sqrt{\nu_1}}{\mathcal{N}_x\sqrt{\eta\alpha}}\ln\mathcal{N}_x\right)^3\left(\frac{\sqrt{\eta\alpha}}{\sqrt{\nu_1}}\right)^4 \le C\mathcal{N}_x^{-3}(\ln\mathcal{N}_x)^3, \quad k = 1, 2, \\
\left\|\mathfrak{R}_k^{n+1/2}\right\|\psi_0\overline{h}^4\theta_1^4 &= \left\|\mathfrak{R}_k^{n+1/2}\right\|\psi_0\left(\frac{16\sqrt{\nu_1}}{\mathcal{N}_x\sqrt{\eta\alpha}}\ln\mathcal{N}_x\right)^4\left(\frac{\sqrt{\eta\alpha}}{\sqrt{\nu_1}}\right)^4 \le C\mathcal{N}_x^{-4}(\ln\mathcal{N}_x)^4, \\
\nu_1\psi_2\overline{h}^2\theta_2^4 &= \nu_1\psi_2\left(\frac{16\sqrt{\nu_1}}{\mathcal{N}_x\sqrt{\eta\alpha}}\ln\mathcal{N}_x\right)^2\left(\frac{\sqrt{\eta\alpha}}{4\sqrt{\nu_1}}\right)^4 \le C\mathcal{N}_x^{-2}(\ln\mathcal{N}_x)^2, \\
\nu_2\left\|p_{kk}^{n+1/2}\right\|\psi_1\overline{h}^3\theta_2^4 &= \nu_2\left\|p_{kk}^{n+1/2}\right\|\psi_1\left(\frac{16\sqrt{\nu_1}}{\mathcal{N}_x\sqrt{\eta\alpha}}\ln\mathcal{N}_x\right)^3\left(\frac{\sqrt{\eta\alpha}}{4\sqrt{\nu_1}}\right)^4 \le C\mathcal{N}_x^{-3}(\ln\mathcal{N}_x)^3, \quad k = 1, 2, \\
\left\|\mathfrak{R}_k^{n+1/2}\right\|\psi_0\overline{h}^4\theta_2^4 &= \left\|\mathfrak{R}_k^{n+1/2}\right\|\psi_0\left(\frac{16\sqrt{\nu_1}}{\mathcal{N}_x\sqrt{\eta\alpha}}\ln\mathcal{N}_x\right)^4\left(\frac{\sqrt{\eta\alpha}}{4\sqrt{\nu_1}}\right)^4 \le C\mathcal{N}_x^{-4}(\ln\mathcal{N}_x)^4, \quad k = 1, 2.
\end{aligned}$$

These inequalities are used in (4.4) and (4.5) to get

$$|\mathcal{L}_1\widetilde{\mathbf{X}}(x_m) - \mathcal{L}_1\mathbf{X}_{\mathcal{N}_x}| \le C\mathcal{N}_x^{-2}(\ln\mathcal{N}_x)^2, \quad 0 \le m \le \frac{\mathcal{N}_x}{4}, \tag{4.6}$$

$$|\mathcal{L}_2\widetilde{\mathbf{X}}(x_m) - \mathcal{L}_2\mathbf{X}_{\mathcal{N}_x}| \le C\mathcal{N}_x^{-2}(\ln \mathcal{N}_x)^2, \quad 0 \le m \le \frac{\mathcal{N}_x}{4}. \tag{4.7}$$

When $x_m \in [\xi_1, 1-\xi_2]$, i.e., $\frac{\mathcal{N}_x}{4} + 1 \le m \le \frac{3\mathcal{N}_x}{4}$, using (4.1), we derive that $\widetilde{\mathbf{X}}$ and its derivatives are bounded in this interval, and using that $\overline{h} \le \frac{2}{\mathcal{N}_x}$ we can obtain

$$|\mathcal{L}_1\widetilde{\mathbf{X}}(x_m) - \mathcal{L}_1\mathbf{X}_{\mathcal{N}_x}| \le C\mathcal{N}_x^{-2}, \quad \frac{\mathcal{N}_x}{4} + 1 \le m \le \frac{3\mathcal{N}_x}{4}, \tag{4.8}$$

and

$$|\mathcal{L}_2\widetilde{\mathbf{X}}(x_m) - \mathcal{L}_2\mathbf{X}_{\mathcal{N}_x}| \le C\mathcal{N}_x^{-2}, \quad \frac{\mathcal{N}_x}{4} + 1 \le m \le \frac{3\mathcal{N}_x}{4}. \tag{4.9}$$

When $x_m \in [1-\xi_2, 1]$, i.e., $\frac{3\mathcal{N}_x}{4} + 1 \le m \le \mathcal{N}_x$, we obtain $\exp(-\theta_1 x_m) \le \exp(-\theta_1(1-\xi_2)) \le \mathcal{N}_x^q$ and $\exp(-\theta_2(1-x_m)) \le 1$. Therefore, (4.2) gives

$$|\mathcal{L}_1\widetilde{\mathbf{X}}(x_m) - \mathcal{L}_1\mathbf{X}_{\mathcal{N}_x}| \le C\left(\nu_1\psi_2\overline{h}^2 + \nu_2\left\|p_{11}^{n+1/2}\right\|\psi_1\overline{h}^3 + \left\|\mathfrak{R}_1^{n+1/2}\right\|\psi_0\overline{h}^4\right)\left(1+\theta_1^4+\theta_2^4\right). \tag{4.10}$$

Also, $\overline{h} = \frac{4\xi_2}{\mathcal{N}_x} = \frac{16\sqrt{\nu_1}}{\mathcal{N}_x\sqrt{\eta\alpha}}\ln \mathcal{N}_x$, so, it holds

$$\nu_1\psi_2\overline{h}^2 = \nu_1\psi_2\left(\frac{16\sqrt{\nu_1}}{\mathcal{N}_x\sqrt{\eta\alpha}}\ln \mathcal{N}_x\right)^2 \le C\mathcal{N}_x^{-2}(\ln \mathcal{N}_x)^2,$$

$$\nu_2\left\|p_{kk}^{n+1/2}\right\|\psi_1\overline{h}^3 = \nu_2\left\|p_{kk}^{n+1/2}\right\|\psi_1\left(\frac{16\sqrt{\nu_1}}{\mathcal{N}_x\sqrt{\eta\alpha}}\ln \mathcal{N}_x\right)^3 \le C\mathcal{N}_x^{-3}(\ln \mathcal{N}_x)^3, \quad k=1,2,$$

$$\left\|\mathfrak{R}_k^{n+1/2}\right\|\psi_0\overline{h}^4 \le C\mathcal{N}_x^{-4}(\ln \mathcal{N}_x)^4, \quad k=1,2,$$

$$\nu_1\psi_2\overline{h}^2\theta_1^4\mathcal{N}_x^q = \nu_1\psi_2\left(\frac{16\sqrt{\nu_1}}{\mathcal{N}_x\sqrt{\eta\alpha}}\ln \mathcal{N}_x\right)^2\left(\frac{\sqrt{\eta\alpha}}{\sqrt{\nu_1}}\right)^4 \le C\mathcal{N}_x^{-2}(\ln \mathcal{N}_x)^2,$$

$$\nu_2\left\|p_{kk}^{n+1/2}\right\|\psi_1\overline{h}^3\theta_1^4 = \nu_2\left\|p_{kk}^{n+1/2}\right\|\psi_1\left(\frac{16\sqrt{\nu_1}}{\mathcal{N}_x\sqrt{\eta\alpha}}\ln \mathcal{N}_x\right)^3\left(\frac{\sqrt{\eta\alpha}}{\sqrt{\nu_1}}\right)^4 \le C\mathcal{N}_x^{-3}(\ln \mathcal{N}_x)^3, \quad k=1,2,$$

$$\left\|\mathfrak{R}_k^{n+1/2}\right\|\psi_0\overline{h}^4\Theta_1^4 = \left\|\mathfrak{R}_k^{n+1/2}\right\|\psi_0\left(\frac{16\sqrt{\nu_1}}{\mathcal{N}_x\sqrt{\eta\alpha}}\ln \mathcal{N}_x\right)^4\left(\frac{\sqrt{\eta\alpha}}{\sqrt{\nu_1}}\right)^4 \le C\mathcal{N}_x^{-4}(\ln \mathcal{N}_x)^4,$$

$$\nu_1\psi_2\overline{h}^2\theta_2^4 = \nu_1\psi_2\left(\frac{16\sqrt{\nu_1}}{\mathcal{N}_x\sqrt{\eta\alpha}}\ln \mathcal{N}_x\right)^2\left(\frac{\sqrt{\eta\alpha}}{4\sqrt{\nu_1}}\right)^4 \le C\mathcal{N}_x^{-2}(\ln \mathcal{N}_x)^2,$$

$$\nu_2\left\|p_{kk}^{n+1/2}\right\|\psi_1\overline{h}^3\theta_2^4 = \nu_2\left\|p_{kk}^{n+1/2}\right\|\psi_1\left(\frac{16\sqrt{\nu_1}}{\mathcal{N}_x\sqrt{\eta\alpha}}\ln \mathcal{N}_x\right)^3\left(\frac{\sqrt{\eta\alpha}}{4\sqrt{\nu_1}}\right)^4 \le C\mathcal{N}_x^{-3}(\ln \mathcal{N}_x)^3, \quad k=1,2,$$

$$\left\|\mathfrak{R}_k^{n+1/2}\right\|\psi_0\overline{h}^4\Theta_2^4 = \left\|\mathfrak{R}_k^{n+1/2}\right\|\psi_0\left(\frac{16\sqrt{\nu_1}}{\mathcal{N}_x\sqrt{\eta\alpha}}\ln \mathcal{N}_x\right)^4\left(\frac{\sqrt{\eta\alpha}}{4\sqrt{\nu_1}}\right)^4 \le C\mathcal{N}_x^{-4}(\ln \mathcal{N}_x)^4, \quad k=1,2.$$

These inequalities from (4.21) are used to get

$$|\mathcal{L}_1\widetilde{\mathbf{X}}(x_m) - \mathcal{L}_1\mathbf{X}_{\mathcal{N}_x}| \le C\mathcal{N}_x^{-2}(\ln \mathcal{N}_x)^2, \quad \frac{3\mathcal{N}_x}{4} + 1 \le m \le \mathcal{N}_x, \tag{4.11}$$

and

$$|\mathcal{L}_2\widetilde{\mathbf{X}}(x_m) - \mathcal{L}_2\mathbf{X}_{\mathcal{N}_x}| \le C\mathcal{N}_x^{-2}(\ln \mathcal{N}_x)^2, \quad \frac{3\mathcal{N}_x}{4} + 1 \le m \le \mathcal{N}_x. \tag{4.12}$$

Combining (4.6)–(4.12) yields

$$|\mathcal{L}\widetilde{\mathbf{X}}(x_m) - \mathcal{L}\mathbf{X}_{\mathcal{N}_x}| \le C\mathcal{N}_x^{-2}(\ln \mathcal{N}_x)^2, \quad 0 \le n \le \mathcal{N}_x, \tag{4.13}$$

$$|\mathcal{L}\mathcal{X}^{n+1} - \mathcal{L}\mathbf{X}_{\mathcal{N}_x}| = |g(x_m) - \mathcal{L}\mathbf{X}_{\mathcal{N}_x}| \le C\mathcal{N}_x^{-2}(\ln \mathcal{N}_x)^2. \tag{4.14}$$

In second case, we consider that $\alpha\nu_2^2 \ge \eta\nu_1$ holds.

Then, if $x_m \in [0, \xi_1]$, i.e., $1 \le m \le \frac{\mathcal{N}_x}{4}$, it holds $\exp(-\theta_1 x_m) \le 1$ and $\exp(-\theta_2(1-x_m)) \le \exp(-\theta_1(1-\xi_1)) \le \mathcal{N}_x^q$. Thus, (4.2) and (4.3) yield

$$|\mathcal{L}_1\widetilde{\mathbf{X}}(x_m) - \mathcal{L}_1\mathbf{X}_{\mathcal{N}_x}| \le C\left(\nu_1\psi_2\overline{h}^2 + \nu_2\left\|p_{11}^{n+1/2}\right\|\psi_1\overline{h}^3 + \left\|\mathfrak{R}_1^{n+1/2}\right\|\psi_0\overline{h}^4\right)(1+\theta_1^4+\theta_2^4), \tag{4.15}$$

and

$$|\mathcal{L}_2\widetilde{\mathbf{X}}(x_m)-\mathcal{L}_2\mathbf{X}_{\mathcal{N}_x}|\le C\left(\nu_1\psi_2\overline{h}^2+\nu_2\left\|p_{22}^{n+1/2}\right\|\psi_1\overline{h}^3+\left\|\mathfrak{R}_2^{n+1/2}\right\|\psi_0\overline{h}^4\right)(1+\theta_1^4+\theta_2^4). \tag{4.16}$$

Also, $\overline{h}=\dfrac{4\xi_1}{\mathcal{N}_x}=\dfrac{16\nu_1}{\mathcal{N}_x\nu_2\alpha}\ln\mathcal{N}_x$, therefore, we have

$$\begin{aligned}
\nu_1\psi_2\overline{h}^2&=\nu_1\psi_2\left(\frac{16\nu_1}{\mathcal{N}_x\nu_2\alpha}\ln\mathcal{N}_x\right)^2\le C\mathcal{N}_x^{-2}(\ln\mathcal{N}_x)^2,\\
\nu_2\left\|p_{kk}^{n+1/2}\right\|\psi_1\overline{h}^3&=\nu_2\left\|p_{kk}^{n+1/2}\right\|\psi_1\left(\frac{16\nu_1}{\mathcal{N}_x\nu_2\alpha}\ln\mathcal{N}_x\right)^3\le C\mathcal{N}_x^{-3}(\ln\mathcal{N}_x)^3,\quad k=1,2,\\
\left\|\mathfrak{R}_k^{n+1/2}\right\|\psi_0\overline{h}^4&\le C\mathcal{N}_x^{-4}(\ln\mathcal{N}_x)^4,\quad k=1,2,\\
\nu_1\psi_2\overline{h}^2\theta_1^4&=\nu_1\psi_2\left(\frac{16\nu_1}{\mathcal{N}_x\nu_2\alpha}\ln\mathcal{N}_x\right)^2\left(\frac{\nu_2\alpha}{\nu_1}\right)^4\le C\mathcal{N}_x^{-2}(\ln\mathcal{N}_x)^2,\\
\nu_2\left\|p_{kk}^{n+1/2}\right\|\psi_1\overline{h}^3\theta_1^4&=\nu_2\left\|p_{kk}^{n+1/2}\right\|\psi_1\left(\frac{16\nu_1}{\mathcal{N}_x\nu_2\alpha}\ln\mathcal{N}_x\right)^3\left(\frac{\nu_2\alpha}{\nu_1}\right)^4\le C\mathcal{N}_x^{-3}(\ln\mathcal{N}_x)^3,\quad k=1,2,\\
\left\|\mathfrak{R}_k^{n+1/2}\right\|\psi_0\overline{h}^4\theta_1^4&=\left\|\mathfrak{R}_k^{n+1/2}\right\|\psi_0\left(\frac{16\nu_1}{\mathcal{N}_x\nu_2\alpha}\ln\mathcal{N}_x\right)^4\left(\frac{\nu_2\alpha}{\nu_1}\right)^4\le C\mathcal{N}_x^{-4}(\ln\mathcal{N}_x)^4,\\
\nu_1\psi_2\overline{h}^2\theta_2^4&=\nu_1\psi_2\left(\frac{16\nu_1}{\mathcal{N}_x\nu_2\alpha}\ln\mathcal{N}_x\right)^2\left(\frac{\eta}{4\nu_2}\right)^4\le C\mathcal{N}_x^{-2}(\ln\mathcal{N}_x)^2,\\
\nu_2\left\|p_{kk}^{n+1/2}\right\|\psi_1\overline{h}^3\theta_2^4&=\nu_2\left\|p_{kk}^{n+1/2}\right\|\psi_1\left(\frac{16\nu_1}{\mathcal{N}_x\nu_2\alpha}\ln\mathcal{N}_x\right)^3\left(\frac{\eta}{4\nu_2}\right)^4\le C\mathcal{N}_x^{-3}(\ln\mathcal{N}_x)^3,\quad k=1,2,\\
\left\|\mathfrak{R}_k^{n+1/2}\right\|\psi_0\overline{h}^4\theta_2^4&=\left\|\mathfrak{R}_k^{n+1/2}\right\|\psi_0\left(\frac{16\nu_1}{\mathcal{N}_x\nu_2\alpha}\ln\mathcal{N}_x\right)^4\left(\frac{\eta}{4\nu_2}\right)^4\le C\mathcal{N}_x^{-4}(\ln\mathcal{N}_x)^4,\quad k=1,2.
\end{aligned}$$

These inequalities are used in (4.4) and (4.5) to get

$$|\mathcal{L}_1\widetilde{\mathbf{X}}(x_m)-\mathcal{L}_1\mathbf{X}_{\mathcal{N}_x}|\le C\mathcal{N}_x^{-2}(\ln\mathcal{N}_x)^2,\quad 0\le m\le\frac{\mathcal{N}_x}{4}, \tag{4.17}$$

$$|\mathcal{L}_2\widetilde{\mathbf{X}}(x_m)-\mathcal{L}_2\mathbf{X}_{\mathcal{N}_x}|\le C\mathcal{N}_x^{-2}(\ln\mathcal{N}_x)^2,\quad 0\le m\le\frac{\mathcal{N}_x}{4}. \tag{4.18}$$

When $x_m\in[\xi_1,1-\xi_2]$,i.e., $\dfrac{\mathcal{N}_x}{4}+1\le m\le\dfrac{3\mathcal{N}_x}{4}$, using (4.1), we derive that $\widetilde{\mathbf{X}}$ and its derivatives are bounded in this interval, and $\overline{h}\le\dfrac{2}{\mathcal{N}_x}$. Then, the local error satisfies

$$|\mathcal{L}_1\widetilde{\mathbf{X}}(x_m)-\mathcal{L}_1\mathbf{X}_{\mathcal{N}_x}|\le C\mathcal{N}_x^{-2},\quad \frac{\mathcal{N}_x}{4}+1\le m\le\frac{3\mathcal{N}_x}{4}, \tag{4.19}$$

and

$$|\mathcal{L}_2\widetilde{\mathbf{X}}(x_m)-\mathcal{L}_2\mathbf{X}_{\mathcal{N}_x}|\le C\mathcal{N}_x^{-2},\quad \frac{\mathcal{N}_x}{4}+1\le m\le\frac{3\mathcal{N}_x}{4}. \tag{4.20}$$

When $x_m\in[1-\xi_2,1]$, i.e., $\dfrac{3\mathcal{N}_x}{4}+1\le m\le\mathcal{N}_x$, we obtain $\exp(-\theta_1x_m)\le\exp(-\theta_1(1-\xi_2))\le\mathcal{N}_x^q$ and $\exp(-\theta_2(1-x_m))\le1$. Therefore, from (4.2) it follows

$$|\mathcal{L}_1\widetilde{\mathbf{X}}(x_m)-\mathcal{L}_1\mathbf{X}_{\mathcal{N}_x}|\le C\left(\nu_1\psi_2\overline{h}^2+\nu_2\left\|p_{11}^{n+1/2}\right\|\psi_1\overline{h}^3+\left\|\mathfrak{R}_1^{n+1/2}\right\|\psi_0\overline{h}^4\right)\left(1+\theta_1^4+\theta_2^4\right). \tag{4.21}$$

Also, $\overline{h}=\dfrac{4\xi_2}{\mathcal{N}_x}=\dfrac{16\nu_2}{\mathcal{N}_x\eta}\ln\mathcal{N}_x$; so, it holds

$$\begin{aligned}
\nu_1\psi_2\overline{h}^2&=\nu_1\psi_2\left(\frac{16\nu_2}{\mathcal{N}_x\eta}\ln\mathcal{N}_x\right)^2\le C\mathcal{N}_x^{-2}(\ln\mathcal{N}_x)^2,\\
\nu_2\left\|p_{kk}^{n+1/2}\right\|\psi_1\overline{h}^3&=\nu_2\left\|p_{kk}^{n+1/2}\right\|\psi_1\left(\frac{16\nu_2}{\mathcal{N}_x\eta}\ln\mathcal{N}_x\right)^3\le C\mathcal{N}_x^{-3}(\ln\mathcal{N}_x)^3,\quad k=1,2,\\
\left\|\mathfrak{R}_k^{n+1/2}\right\|\psi_0\overline{h}^4&\le C\mathcal{N}_x^{-4}(\ln\mathcal{N}_x)^4,\quad k=1,2,\\
\nu_1\psi_2\overline{h}^2\theta_1^4\mathcal{N}_x^q&=\nu_1\psi_2\left(\frac{16\nu_2}{\mathcal{N}_x\eta}\ln\mathcal{N}_x\right)^2\left(\frac{\nu_2\alpha}{\nu_1}\right)^4\le C\mathcal{N}_x^{-2}(\ln\mathcal{N}_x)^2,\\
\nu_2\left\|p_{kk}^{n+1/2}\right\|\psi_1\overline{h}^3\theta_1^4&=\nu_2\left\|p_{kk}^{n+1/2}\right\|\psi_1\left(\frac{16\nu_2}{\mathcal{N}_x\eta}\ln\mathcal{N}_x\right)^3\left(\frac{\alpha\nu_2}{\nu_1}\right)^4\le C\mathcal{N}_x^{-3}(\ln\mathcal{N}_x)^3,\quad k=1,2,
\end{aligned}$$

$$\left\|\mathfrak{R}_k^{n+1/2}\right\|\psi_0\overline{h}^4\theta_1^4 = \left\|\mathfrak{R}_k^{n+1/2}\right\|\psi_0\left(\frac{16\nu_2}{\mathcal{N}_x\eta}\ln\mathcal{N}_x\right)^4\left(\frac{\nu_2\alpha}{\nu_1}\right)^4 \le C\mathcal{N}_x^{-4}(\ln\mathcal{N}_x)^4,$$

$$\nu_1\psi_2\overline{h}^2\theta_2^4 = \nu_1\psi_2\left(\frac{16\nu_2}{\mathcal{N}_x\eta}\ln\mathcal{N}_x\right)^2\left(\frac{\eta}{4\nu_2}\right)^4 \le C\mathcal{N}_x^{-2}(\ln\mathcal{N}_x)^2,$$

$$\nu_2\left\|p_{kk}^{n+1/2}\right\|\psi_1\overline{h}^3\theta_2^4 = \nu_2\left\|p_{kk}^{n+1/2}\right\|\psi_1\left(\frac{16\nu_2}{\mathcal{N}_x\eta}\ln\mathcal{N}_x\right)^3\left(\frac{\eta}{4\nu_2}\right)^4 \le C\mathcal{N}_x^{-3}(\ln\mathcal{N}_x)^3, \quad k=1,2,$$

$$\left\|\mathfrak{R}_k^{n+1/2}\right\|\psi_0\overline{h}^4\Theta_2^4 = \left\|\mathfrak{R}_k^{n+1/2}\right\|\psi_0\left(\frac{16\nu_2}{\mathcal{N}_x\eta}\ln\mathcal{N}_x\right)^4\left(\frac{\eta}{4\nu_2}\right)^4 \le C\mathcal{N}_x^{-4}(\ln\mathcal{N}_x)^4, \quad k=1,2.$$

These inequalities from (4.21) are used to get

$$|\mathcal{L}_1\widetilde{\mathbf{X}}(x_m) - \mathcal{L}_1\mathbf{X}_{\mathcal{N}_x}| \le C\mathcal{N}_x^{-2}(\ln\mathcal{N}_x)^2, \quad \frac{3\mathcal{N}_x}{4}+1 \le m \le \mathcal{N}_x, \tag{4.22}$$

and

$$|\mathcal{L}_2\widetilde{\mathbf{X}}(x_m) - \mathcal{L}_2\mathbf{X}_{\mathcal{N}_x}| \le C\mathcal{N}_x^{-2}(\ln\mathcal{N}_x)^2, \quad \frac{3\mathcal{N}_x}{4}+1 \le m \le \mathcal{N}_x. \tag{4.23}$$

Combining (4.17)–(4.23) yields

$$|\mathcal{L}\widetilde{\mathbf{X}}(x_m) - \mathcal{L}\mathbf{X}_{\mathcal{N}_x}| \le C\mathcal{N}_x^{-2}(\ln\mathcal{N}_x)^2, \quad 0 \le n \le \mathcal{N}_x, \tag{4.24}$$

$$|\mathcal{L}\mathcal{X}^{n+1} - \mathcal{L}\mathbf{X}_{\mathcal{N}_x}| = |g(x_m) - \mathcal{L}\mathbf{X}_{\mathcal{N}_x}| \le C\mathcal{N}_x^{-2}(\ln\mathcal{N}_x)^2. \tag{4.25}$$

Now, for both cases, let $\widehat{\mathcal{L}}\mathbf{X}_{\mathcal{N}_x}(x) = \tilde{g}(x_m)$, $\mathbf{X}_{\mathcal{N}_x}(x_0) = \mathfrak{l}_1(s_{n+1})$, $\mathbf{X}_{\mathcal{N}_x}(x_{\mathcal{N}_x}) = \mathfrak{m}_1(s_{n+1})$, which results in the linear system

$$\mathcal{A}\widetilde{\mathbf{w}}^{n+1} = \widetilde{\mathcal{B}}.$$

Next, it follows

$$\mathcal{A}(\mathbf{w}^{n+1} - \widetilde{\mathbf{w}}^{n+1}) = \mathcal{B} - \widetilde{\mathcal{B}}, \tag{4.26}$$

where

$$\mathbf{w}^{n+1} - \widetilde{\mathbf{w}}^{n+1} = (w_{0;1}^{n+1} - \widetilde{w}_{0;1}^{n+1}, w_1^{n+1}; 1 - \widetilde{w}_1^{n+1}; 1, \ldots, w_{\mathcal{N}_x;1}^{n+1} - \widetilde{w}_{\mathcal{N}_x;1}^{n+1}, w_{0;2}^{n+1} - \widetilde{w}_{0;2}^{n+1}, \ldots, w_{\mathcal{N}_x;2}^{n+1} - \widetilde{w}_{\mathcal{N}_x;2}^{n+1})^T,$$

$$\mathcal{B} - \widetilde{\mathcal{B}} = (g_1(x_0) - \tilde{g}_1(x_0), g_1(x_1) - \tilde{g}_1(x_1), \ldots, g_1(x_{\mathcal{N}_x}) - \tilde{g}_1(x_{\mathcal{N}_x}), g_2(x_0) - \tilde{g}_2(x_0), \ldots, g_2(x_{\mathcal{N}_x}) - \tilde{g}_2(x_{\mathcal{N}_x}))^T.$$

Therefore, using (4.14) and (4.25), we get

$$\|\mathcal{B} - \widetilde{\mathcal{B}}\| \le C\mathcal{N}_x^{-2}(\ln\mathcal{N}_x)^2. \tag{4.27}$$

Utilizing this estimate, from [29], (4.26) and (4.27), we deduce that it holds

$$\|\mathbf{w}^{n+1} - \widetilde{\mathbf{w}}^{n+1}\| \le \|\mathcal{A}^{-1}\|\|\mathcal{B} - \widetilde{\mathcal{B}}\| \le C\mathcal{N}_x^{-2}(\ln\mathcal{N}_x)^2. \tag{4.28}$$

The system matrix $\mathcal{A}$ arising in (4.26) is a block tridiagonal and strictly diagonally dominant matrix. Hence, $\mathcal{A}$ is an M-matrix (see, e.g., [29]), which guarantees that $\mathcal{A}^{-1}$ exists and is nonnegative. Moreover, letting

$$\delta := \min_i\Big(a_{ii} - \sum_{j\ne i}|a_{ij}|\Big),$$

the strict diagonal dominance of the reaction matrix Q yields $\delta \ge C_0 > 0$, where C_0 is independent of the perturbation parameters ν_1, ν_2 and the discretization parameter $\mathcal{N}_x$. Consequently, it holds

$$\|\mathcal{A}^{-1}\|_\infty \le \frac{1}{\delta} \le C,$$

for some constant C independent of ν_1, ν_2 and $\mathcal{N}_x$. This establishes the desired uniform bound for $\mathcal{A}^{-1}$.

From (3.6c)–(3.6f) as boundary conditions, we get

$$|w_{-1}^{n+1} - \widetilde{w}_{-1}^{n+1}| \le C\mathcal{N}_x^{-2}(\ln\mathcal{N}_x)^2,$$

and

$$|w_{\mathcal{N}_x+1}^{n+1} - \widetilde{w}_{\mathcal{N}_x+1}^{n+1}| \le C\mathcal{N}_x^{-2}(\ln\mathcal{N}_x)^2,$$

and thus

$$\max_{-1\le m\le\mathcal{N}_x+1}|w_m^{n+1} - \widetilde{w}_m^{n+1}| \le C\mathcal{N}_x^{-2}(\ln\mathcal{N}_x)^2.$$

Hence, we have

$$|\mathcal{X}^{n+1} - \mathbf{X}_{\mathcal{N}_x}(x)| \le \max_{-1\le m\le\mathcal{N}_x+1}|w_m^{n+1} - \widetilde{w}_m^{n+1}|\sum_{m=-1}^{\mathcal{N}_x+1}|D_m(x)| \le C\mathcal{N}_x^{-2}(\ln\mathcal{N}_x)^2,$$

Table 2
$E^{\mathcal{N}_x,\mathcal{N}_s}_{1,\nu_1,\nu_2}$, $R^{\mathcal{N}_x,\mathcal{N}_s}_{1,\nu_1,\nu_2}$, $E^{\mathcal{N}_x,\mathcal{N}_s}_{1,\nu_1}$, $R^{\mathcal{N}_x,\mathcal{N}_s}_{1,\nu_1}$ for Example 5.1 taking $\nu_1 = 2^{-8}$.

ν_2	$(\mathcal{N}_x, \mathcal{N}_s) \rightarrow$				
	(12, 6)	(24, 12)	(48, 24)	(96, 48)	(192, 96)
2^{-6}	4.0105e−04	1.4520e−04	4.5998e−05	1.25189e−05	3.1997e−06
	1.4657	1.6584	1.8775	1.9681	
2^{-10}	4.0045e−04	1.4460e−04	4.5983e−05	1.25143e−05	3.1983e−06
	1.4696	1.6529	1.8775	1.9682	
2^{-14}	4.0238e−04	1.4538e−04	4.6103e−05	1.3426e−05	3.3889e−06
	1.4687	1.6569	1.7798	1.9861	
2^{-18}	4.0289e−04	1.4541e−04	4.6109e−05	1.3428e−05	3.3893e−06
	1.4703	1.6570	1.7798	1.9862	
2^{-22}	4.0293e−04	1.4541e−04	4.6110e−05	1.3429e−05	3.3893e−06
	1.4704	1.6570	1.7797	1.9863	
2^{-26}	4.0293e−04	1.4541e−04	4.6110e−05	1.3429e−05	3.3893e−06
	1.4704	1.6570	1.7797	1.9863	
$E^{\mathcal{N}_x,\mathcal{N}_s}_{1,\nu_1}$	4.0293e−04	1.4541e−04	4.6110e−05	1.3429e−05	3.3893e−06
$R^{\mathcal{N}_x,\mathcal{N}_s}_{1,\nu_1}$	1.4704	1.6570	1.7797	1.9863	
CPU time (s)	0.0620	0.0814	0.0902	0.4532	0.9290

Table 3
$E^{\mathcal{N}_x,\mathcal{N}_s}_{2,\nu_1,\nu_2}$, $R^{\mathcal{N}_x,\mathcal{N}_s}_{2,\nu_1,\nu_2}$, $E^{\mathcal{N}_x,\mathcal{N}_s}_{2,\nu_1}$, $R^{\mathcal{N}_x,\mathcal{N}_s}_{2,\nu_1}$ for Example 5.1 taking $\nu_1 = 2^{-8}$.

	$(\mathcal{N}_x, \mathcal{N}_s) \rightarrow$				
ν_2	(12, 6)	(24, 12)	(48, 24)	(96, 48)	(192, 96)
2^{-6}	1.6316e−04	5.4838e−05	1.5829e−05	4.2841e−06	1.0979e−06
	1.5730	1.7926	1.8855	1.9642	
2^{-10}	1.6137e−04	5.4642e−05	1.5770e−05	4.2692e−06	1.0821e−06
	1.5623	1.7928	1.8851	1.9801	
2^{-14}	1.6365e−04	5.4702e−05	1.5850e−05	4.2801e−06	1.0910e−06
	1.5809	1.7871	1.8888	1.9720	
2^{-18}	1.6465e−04	5.4714e−05	1.5854e−05	4.2810e−06	1.0914e−06
	1.5894	1.7871	1.8888	1.9718	
2^{-22}	1.6467e−04	5.4714e−05	1.5855e−05	4.2811e−06	1.0914e−06
	1.5896	1.7870	1.8889	1.9718	
2^{-26}	1.6467e−04	5.4714e−05	1.5855e−05	4.2811e−06	1.0914e−06
	1.5896	1.7870	1.8889	1.9718	
$E^{\mathcal{N}_x,\mathcal{N}_s}_{2,\nu_1}$	1.6467e−04	5.4714e−05	1.5855e−05	4.2811e−06	1.0914e−06
$R^{\mathcal{N}_x,\mathcal{N}_s}_{2,\nu_1}$	1.5896	1.7870	1.8889	1.9718	
CPU time (s)	0.0710	0.0921	0.1092	0.4618	0.9781

which provides

$$\max_{0\le m\le \mathcal{N}_x} |\mathcal{X}^{n+1} - \mathbf{X}_{\mathcal{N}_x}(x)| \le C\mathcal{N}_x^{-2}(\ln \mathcal{N}_x)^2.$$

Thus, using the triangle inequality leads to

$$\sup_{0<\nu_1,\nu_2\le 1} \|\mathcal{X}^{n+1} - \widetilde{\mathbf{X}}^{n+1}\| \le C\mathcal{N}_x^{-2}(\ln \mathcal{N}_x)^2,$$

which is the required result. □

Using the previous results, we can obtain the main result of the work, which proves the uniform convergence of the fully discrete scheme.

Theorem 4.3. *The error associated to the numerical solution $\mathcal{X}^{n+1}$ given by the fully discretized scheme (3.8) on the piecewise uniform Shishkin mesh, satisfies*

$$\sup_{0<\nu_1,\nu_2\le 1} \|\mathbf{X} - \mathcal{X}\| \le C((\Delta s)^{3/2} + \mathcal{N}_x^{-2+p}(\ln \mathcal{N}_x)^2),$$

where $0 < p < 1$ and $\mathcal{N}_x^{-p} \le \Delta s$. Therefore, the fully discrete scheme is a uniformly convergent method which has second order of convergence in time and almost second order in space.

Table 4
$E^{\mathcal{N}_x,\mathcal{N}_s}_{1,\nu_1,\nu_2}$, $R^{\mathcal{N}_x,\mathcal{N}_s}_{1,\nu_1,\nu_2}$, $E^{\mathcal{N}_x,\mathcal{N}_s}_{1,\nu_2}$, $R^{\mathcal{N}_x,\mathcal{N}_s}_{1,\nu_2}$ for Example 5.1 taking $\nu_2 = 2^{-8}$.

	$(\mathcal{N}_x, \mathcal{N}_s) \rightarrow$				
ν_1	(12, 6)	(24, 12)	(48, 24)	(96, 48)	(192, 96)
2^{-19}	2.8702e−04	8.7851e−05	2.4431e−05	6.6963e−06	1.6789e−06
	1.7080	1.8463	1.8673	1.9958	
2^{-21}	2.8794e−04	8.7928e−05	2.4512e−05	6.6704e−06	1.6677e−06
	1.7114	1.8428	1.8776	1.9999	
2^{-23}	2.8795e−04	8.7927e−05	2.4507e−05	6.6999e−06	1.6672e−06
	1.7114	1.8431	1.8710	2.0067	
2^{-25}	2.8795e−04	8.7924e−05	2.4506e−05	6.6999e−06	1.6673e−06
	1.7115	1.8431	1.8709	2.0066	
2^{-27}	2.8795e−04	8.7924e−05	2.4506e−05	6.6999e−06	1.6673e−06
	1.7115	1.8431	1.8709	2.0066	
2^{-29}	2.8795e−04	8.7924e−05	2.4506e−05	6.6999e−06	1.6673e−06
	1.7115	1.8431	1.8709	2.0066	
$E^{\mathcal{N}_x,\mathcal{N}_s}_{1,\nu_2}$	2.8795e−04	8.7924e−05	2.4506e−05	6.6999e−06	1.6673e−06
$R^{\mathcal{N}_x,\mathcal{N}_s}_{1,\nu_2}$	1.7115	1.8431	1.8709	2.0066	
CPU time (s)	0.0623	0.0849	0.1028	0.5180	0.9801

Table 5
$E^{\mathcal{N}_x,\mathcal{N}_s}_{2,\nu_1,\nu_2}$, $R^{\mathcal{N}_x,\mathcal{N}_s}_{2,\nu_1,\nu_2}$, $E^{\mathcal{N}_x,\mathcal{N}_s}_{2,\nu_2}$, $R^{\mathcal{N}_x,\mathcal{N}_s}_{2,\nu_2}$ for Example 5.1 taking $\nu_2 = 2^{-8}$.

	$(\mathbb{N}_s, \mathcal{N}_x) \rightarrow$				
ν_1	(12, 6)	(24, 12)	(48, 24)	(96, 48)	(192, 96)
2^{-19}	1.9779e−04	7.0635e−05	2.4179e−05	7.7136e−06	2.0106e−06
	1.4855	1.5466	1.6483	1.9398	
2^{-21}	1.9781e−04	7.0634e−05	2.4211e−05	7.7147e−06	2.0108e−06
	1.4857	1.5447	1.6500	1.9398	
2^{-23}	1.9783e−04	7.0635e−05	2.4212e−05	7.7148e−06	2.0109e−06
	1.4858	1.5447	1.6500	1.9398	
2^{-25}	1.9784e−04	7.0637e−05	2.4212e−05	7.7149e−06	2.0109e−06
	1.4858	1.5447	1.6500	1.9398	
2^{-27}	1.9784e−04	7.0637e−05	2.4212e−05	7.7149e−06	2.0109e−06
	1.4858	1.5447	1.6500	1.9398	
2^{-29}	1.9784e−04	7.0637e−05	2.4212e−05	7.7149e−06	2.0109e−06
	1.4858	1.5447	1.6500	1.9398	
$E^{\mathcal{N}_x,\mathcal{N}_s}_{2,\nu_2}$	1.9784e−04	7.0637e−05	2.4212e−05	7.7149e−06	2.0109e−06
$R^{\mathcal{N}_x,\mathcal{N}_s}_{2,\nu_2}$	1.4858	1.5447	1.6500	1.9398	
CPU time (s)	0.0568	0.0639	0.0792	0.1882	0.6851

Table 6
$E^{\mathcal{N}_x,\mathcal{N}_s}_{1,\nu_1,\nu_2}$, $R^{\mathcal{N}_x,\mathcal{N}_s}_{1,\nu_1,\nu_2}$, $E^{\mathcal{N}_x,\mathcal{N}_s}_{1,\nu_1}$, $R^{\mathcal{N}_x,\mathcal{N}_s}_{1,\nu_1}$ for Example 5.1 taking $\nu_1 = 2^{-8}$.

	$(\mathcal{N}_x, \mathcal{N}_s) \rightarrow$				
ν_2	(12, 6)	(48, 12)	(192, 24)	(768, 48)	(3072, 96)
2^{-6}	4.0105e−04	1.2125e−04	3.4282e−05	8.5983e−06	2.1527e−06
	1.7258	1.8225	1.9953	1.9979	
2^{-10}	4.0045e−04	1.2121e−04	3.3287e−05	8.3584e−06	2.0837e−06
	1.7241	1.8645	1.8775	2.0041	
2^{-14}	4.0238e−04	1.2508e−04	3.3307e−05	8.3586e−06	2.0919e−06
	1.6857	1.9090	1.9945	1.9984	
2^{-18}	4.0289e−04	1.2508e−04	3.3409e−05	8.3608e−06	2.0921e−06
	1.6875	1.9045	1.9985	1.9987	
2^{-22}	4.0293e−04	1.2508e−04	3.3410e−05	8.3609e−06	2.0921e−06
	1.6877	1.9045	1.9985	1.9987	
2^{-26}	4.0293e−04	1.2508e−04	3.3410e−05	8.3609e−06	2.0921e−06
	1.6877	1.9045	1.9985	1.9987	
$E^{\mathcal{N}_x,\mathcal{N}_s}_{1,\nu_1}$	4.0293e−04	1.2508e−04	3.3410e−05	8.3609e−06	2.0921e−06
$R^{\mathcal{N}_x,\mathcal{N}_s}_{1,\nu_1}$	1.6877	1.9045	1.9985	1.9987	
CPU time (s)	0.0620	0.0974	0.1336	0.3512	0.5190

Table 7
$E^{\mathcal{N}_x,\mathcal{N}_s}_{1,\nu_1,\nu_2}$, $R^{\mathcal{N}_x,\mathcal{N}_s}_{1,\nu_1,\nu_2}$, $E^{\mathcal{N}_x,\mathcal{N}_s}_{1,\nu_1}$, $R^{\mathcal{N}_x,\mathcal{N}_s}_{1,\nu_1}$ for Example 5.2 taking $\nu_1 = 2^{-8}$.

	$(\mathcal{N}_x, \mathcal{N}_s) \rightarrow$				
ν_2	(12, 6)	(24, 12)	(48, 24)	(96, 48)	(192, 96)
2^{-6}	6.0117e−04	2.1023e−04	6.1972e−05	1.75621e−05	4.7197e−06
	1.5158	1.7623	1.8192	1.8957	
2^{-10}	6.0137e−04	2.1035e−04	6.1986e−05	1.75633e−05	4.7206e−06
	1.5155	1.7628	1.8194	1.8955	
2^{-14}	6.0259e−04	2.1206e−04	6.2087e−05	1.75737e−05	4.7372e−06
	1.5067	1.7721	1.8209	1.8913	
2^{-18}	6.0267e−04	2.1209e−04	6.2088e−05	1.75738e−05	4.7372e−06
	1.5067	1.7723	1.8209	1.8913	
2^{-22}	6.0269e−04	2.1211e−04	6.2089e−05	1.75738e−05	4.7372e−06
	1.5066	1.7724	1.8209	1.8913	
2^{-26}	6.0269e−04	2.1211e−04	6.2089e−05	1.75738e−05	4.7372e−06
	1.5066	1.7724	1.8209	1.8913	
$E^{\mathcal{N}_x,\mathcal{N}_s}_{1,\nu_1}$	6.0269e−04	2.1211e−04	6.2089e−05	1.75738e−05	4.7372e−06
$R^{\mathcal{N}_x,\mathcal{N}_s}_{1,\nu_1}$	1.5066	1.7724	1.8209	1.8913	
CPU time (s)	0.0831	0.0976	0.1073	0.8318	1.2973

Table 8
$E^{\mathcal{N}_x,\mathcal{N}_s}_{2,\nu_1,\nu_2}$, $R^{\mathcal{N}_x,\mathcal{N}_s}_{2,\nu_1,\nu_2}$, $E^{\mathcal{N}_x,\mathcal{N}_s}_{2,\nu_1}$, $R^{\mathcal{N}_x,\mathcal{N}_s}_{2,\nu_1}$ for Example 5.2 taking $\nu_1 = 2^{-8}$.

	$(\mathcal{N}_x, \mathcal{N}_s) \rightarrow$				
ν_2	(12, 6)	(24, 12)	(48, 24)	(96, 48)	(192, 96)
2^{-6}	3.1650e−04	1.1021e−04	3.2378e−05	8.75641e−06	2.2213e−06
	1.5220	1.7672	1.8866	1.9789	
2^{-10}	3.1639e−04	1.1012e−04	3.2371e−05	8.75633e−06	2.2206e−06
	1.5226	1.7663	1.8863	1.9794	
2^{-14}	3.1742e−04	1.1124e−04	3.2482e−05	8.75735e−06	2.2308e−06
	1.5127	1.7760	1.8911	1.9729	
2^{-18}	3.1752e−04	1.1132e−04	3.2489e−05	8.75742e−06	2.2314e−06
	1.5121	1.7767	1.8914	1.9726	
2^{-22}	3.1754e−04	1.1133e−04	3.2491e−05	8.75743e−06	2.2316e−06
	1.5121	1.7767	1.8915	1.9724	
2^{-26}	3.1754e−04	1.1133e−04	3.2491e−05	8.75743e−06	2.2316e−06
	1.5121	1.7767	1.8915	1.9724	
$E^{\mathcal{N}_x,\mathcal{N}_s}_{2,\nu_1}$	3.1754e−04	1.1133e−04	3.2491e−05	8.75743e−06	2.2316e−06
$R^{\mathcal{N}_x,\mathcal{N}_s}_{2,\nu_1}$	1.5121	1.7767	1.8915	1.9724	
CPU time (s)	0.0593	0.0639	0.0801	1.0541	1.1261

Table 9
$E^{\mathcal{N}_x,\mathcal{N}_s}_{1,\nu_1,\nu_2}$, $R^{\mathcal{N}_x,\mathcal{N}_s}_{1,\nu_1,\nu_2}$, $E^{\mathcal{N}_x,\mathcal{N}_s}_{1,\nu_2}$, $R^{\mathcal{N}_x,\mathcal{N}_s}_{1,\nu_2}$ for Example 5.2 taking $\nu_2 = 2^{-8}$.

	$(\mathcal{N}_x, \mathcal{N}_s) \rightarrow$				
ν_1	(12, 6)	(24, 12)	(48, 24)	(96, 48)	(192, 96)
2^{-19}	2.9839e−04	9.2962e−05	2.9605e−05	8.3098e−06	1.9329e−06
	1.6825	1.6508	1.8330	2.1040	
2^{-21}	2.9845e−04	9.3038e−05	2.6633e−05	7.3159e−06	1.9374e−06
	1.6816	1.8046	1.8641	1.9169	
2^{-23}	2.9862e−04	9.3045e−05	2.6636e−05	7.5163e−06	1.9377e−06
	1.6823	1.8046	1.8253	1.9557	
2^{-25}	2.9863e−04	9.3045e−05	2.6638e−05	7.5164e−06	1.9377e−06
	1.6824	1.8044	1.8254	1.9557	
2^{-27}	2.9863e−04	9.3045e−05	2.6638e−05	7.5164e−06	1.9377e−06
	1.6824	1.8044	1.8254	1.9557	
2^{-29}	2.9863e−04	9.3045e−05	2.6638e−05	7.5164e−06	1.9377e−06
	1.6824	1.8044	1.8254	1.9557	
$E^{\mathcal{N}_x,\mathcal{N}_s}_{1,\nu_2}$	2.9863e−04	9.3045e−05	2.6638e−05	7.5164e−06	1.9377e−06
$R^{\mathcal{N}_x,\mathcal{N}_s}_{1,\nu_2}$	1.6824	1.8044	1.8254	1.9557	
CPU time (s)	0.0823	0.0987	0.4843	0.9184	1.3285

Table 10
$E^{\mathcal{N}_x,\mathcal{N}_s}_{2,\nu_1,\nu_2}$, $R^{\mathcal{N}_x,\mathcal{N}_s}_{2,\nu_1,\nu_2}$, $E^{\mathcal{N}_x,\mathcal{N}_s}_{2,\nu_2}$, $R^{\mathcal{N}_x,\mathcal{N}_s}_{2,\nu_2}$ for Example 5.2 taking $\nu_2 = 2^{-8}$.

	$(\mathbb{N}_s, \mathcal{N}_x) \rightarrow$				
ν_1	(12, 6)	(24, 12)	(48, 24)	(96, 48)	(192, 96)
2^{-19}	4.1872e−04	1.4371e−04	4.4658e−05	1.2792e−05	3.335e−06
	1.5428	1.6862	1.8037	1.9395	
2^{-21}	4.1947e−04	1.4429e−04	4.4735e−05	1.2891e−05	3.3381e−06
	1.5396	1.6895	1.7950	1.9493	
2^{-23}	4.1953e−04	1.4435e−04	4.4740e−05	1.2894e−05	3.3381e−06
	1.5392	1.6899	1.7949	1.9496	
2^{-25}	4.1955e−04	1.4436e−04	4.4742e−05	1.2895e−05	3.3382e−06
	1.5392	1.6900	1.7948	1.9497	
2^{-27}	4.1955e−04	1.4436e−04	4.4742e−05	1.2895e−05	3.3382e−06
	1.5392	1.6900	1.7948	1.9497	
2^{-29}	4.1955e−04	1.4436e−04	4.4742e−05	1.2895e−05	3.3382e−06
	1.5392	1.6900	1.7948	1.9497	
$E^{\mathcal{N}_x,\mathcal{N}_s}_{2,\nu_2}$	4.1955e−04	1.4436e−04	4.4742e−05	1.2895e−05	3.3382e−06
$R^{\mathcal{N}_x,\mathcal{N}_s}_{2,\nu_2}$	1.5392	1.6900	1.7948	1.9497	
CPU time (s)	0.0692	0.0726	0.1054	0.6238	1.0947

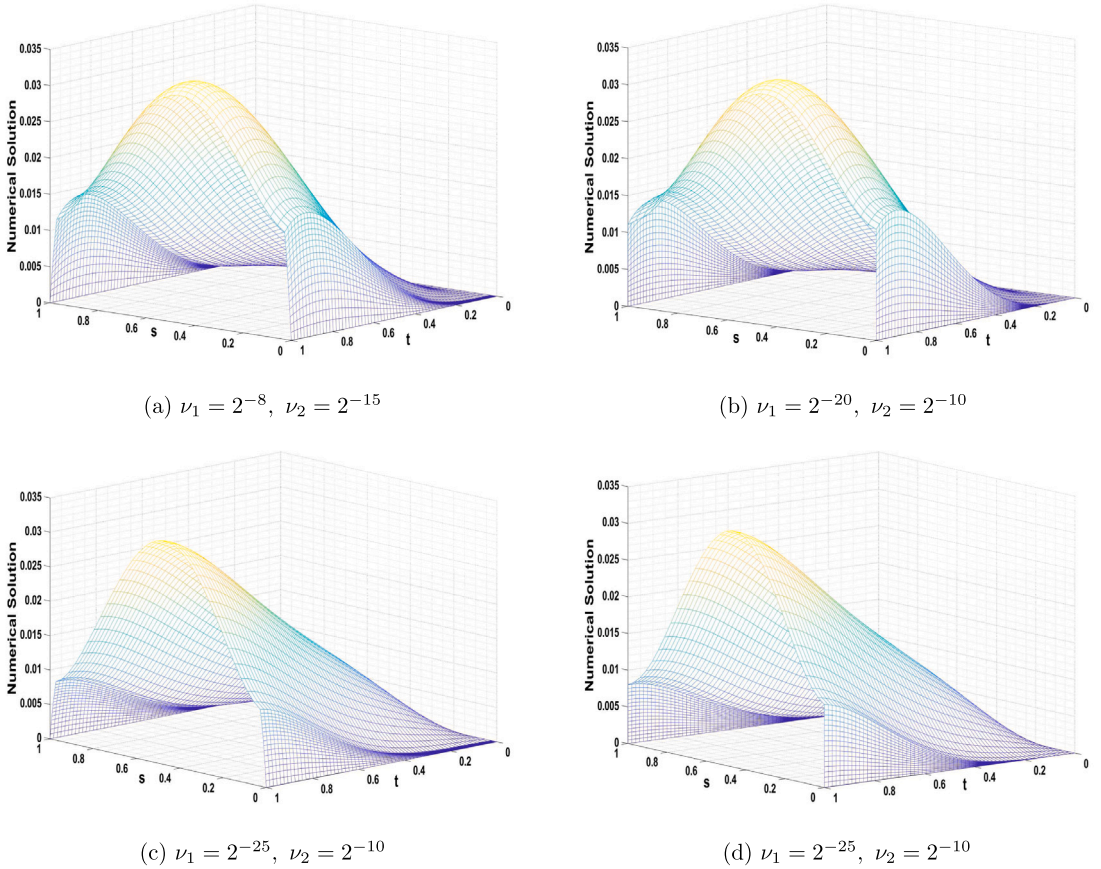

(a) $\nu_1 = 2^{-8},\ \nu_2 = 2^{-15}$ (b) $\nu_1 = 2^{-20},\ \nu_2 = 2^{-10}$

(c) $\nu_1 = 2^{-25},\ \nu_2 = 2^{-10}$ (d) $\nu_1 = 2^{-25},\ \nu_2 = 2^{-10}$

Fig. 1. Surface plots for Example 5.1's first and second solution components using various values of ν_1 and ν_2 with $\mathcal{N}_x = \mathcal{N}_s = 72$.

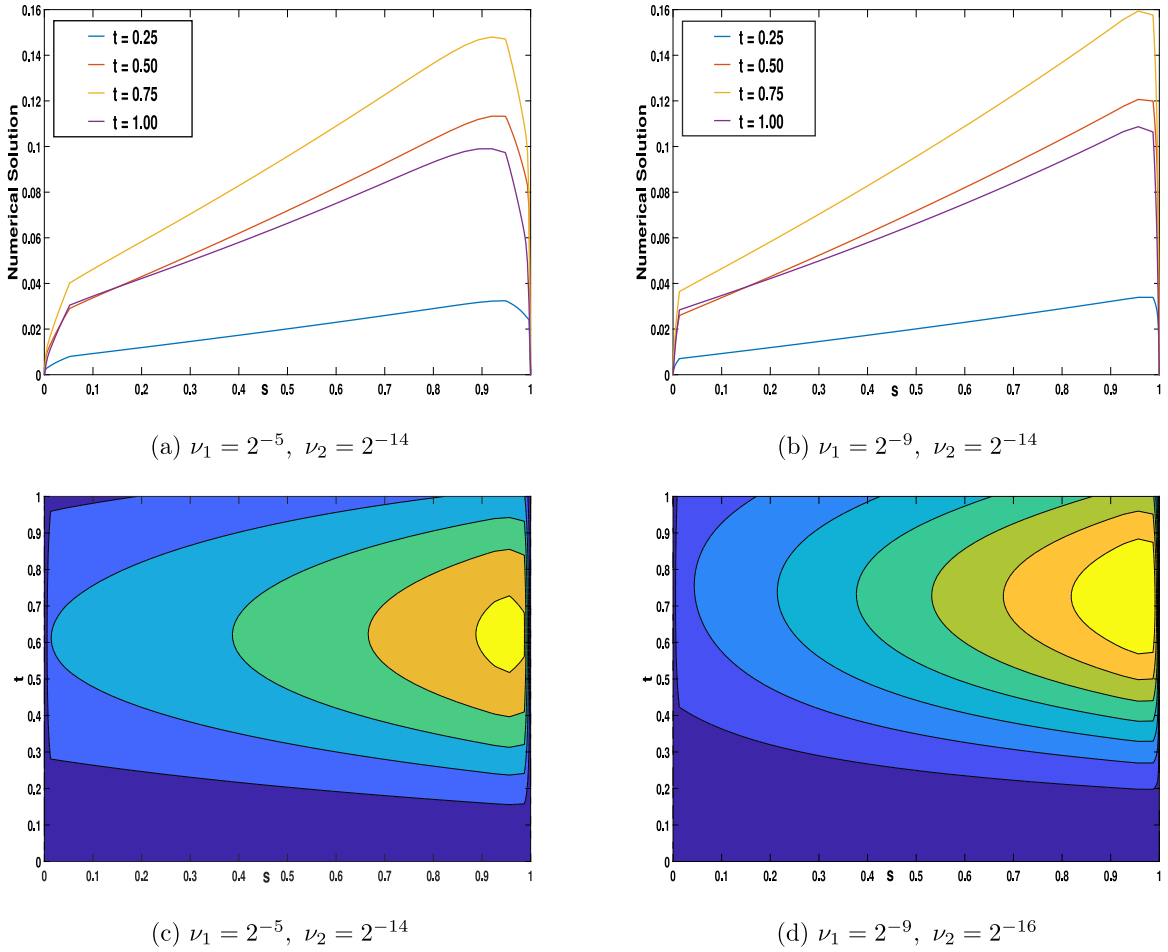

(a) $\nu_1 = 2^{-5},\ \nu_2 = 2^{-14}$ (b) $\nu_1 = 2^{-9},\ \nu_2 = 2^{-14}$

(c) $\nu_1 = 2^{-5},\ \nu_2 = 2^{-14}$ (d) $\nu_1 = 2^{-9},\ \nu_2 = 2^{-16}$

Fig. 2. For the first solution component of Example 5.1, numerical solution at various time levels ((a) and (b)) using various values of ν_1 and ν_2, and contour plots ((c) and (d)) of the solution using $\mathcal{N}_x = \mathcal{N}_s = 72$.

Proof. This result is established by combining the findings of Lemma 3.1 and Theorem 4.2 and following a similar technique that this one in [1]. □

Remark 4.4. From previous Theorem, we see that the order in space is reduced by the value of the constant q; nevertheless, as we will see in the numerical results section, this reduction occurs only from a theoretical point of view, due to the technique used to prove the uniform convergence of the fully discrete scheme. In practice, this reduction does not appear and the real order of uniform convergence is almost two due only to the logarithmic factor, which is an usual factor when piecewise uniform Shishkin meshes are used to solve singularly perturbed problems.

5. Numerical results

Example 5.1.

$$\begin{cases} \dfrac{\partial X_1}{\partial s} - \nu_1 \dfrac{\partial^2 X_1}{\partial x^2} - 7\nu_2 \dfrac{\partial X_1}{\partial x} + (3+x)X_1 - 6X_2 = -X_1(x, s-0.5) + s^3(1-s), \\ \dfrac{\partial X_2}{\partial s} - \nu_1 \dfrac{\partial^2 X_2}{\partial x^2} - 7\nu_2 \dfrac{\partial X_2}{\partial x} - 2X_1 + (5+e^x)X_2 = -X_1(x, s-0.5) + x^2(1-x)^2, \\ X_1(x,s) = 0,\ X_2(x,s) = 0,\ (x,s) \in \mathcal{M}_b \\ X_1(0,s) = 0,\ X_1(1,s) = 0,\ X_2(0,s) = 0,\ X_2(1,s) = 0,\ s \in [0,1]. \end{cases}$$

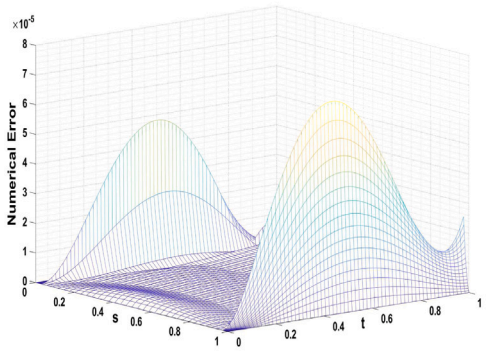

(a) First component with $\mathcal{N}_x = \mathcal{N}_s = 32$

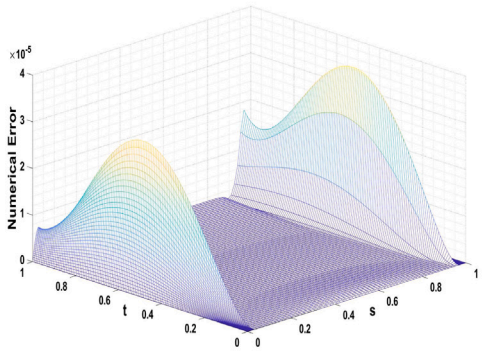

(b) First component with $\mathcal{N}_x = \mathcal{N}_s = 64$

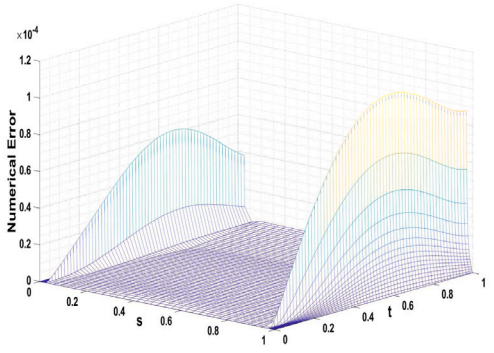

(c) Second component with $\mathcal{N}_x = \mathcal{N}_s = 16$

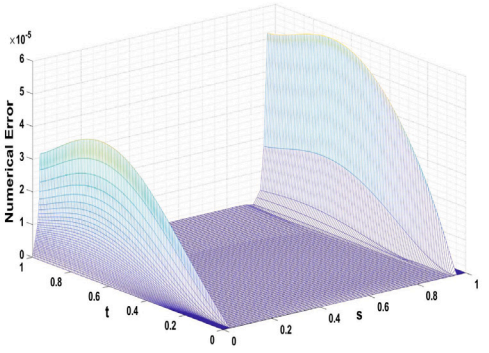

(d) Second component with $\mathcal{N}_x = \mathcal{N}_s = 32$

Fig. 3. Error graphs for Example 5.1's solution components using $\nu_1 = 2^{-10}$ and $\nu_2 = 2^{-15}$.

Example 5.2.

$$\begin{cases} \dfrac{\partial X_1}{\partial s} - \nu_1 \dfrac{\partial^2 X_1}{\partial x^2} - \nu_2 \left(1 + x^2 + \dfrac{\sin(\pi x)}{2}\right) \dfrac{\partial X_1}{\partial x} + 2(1+s)^2 X_1 - (1+s^3) X_2 = -2X_1(x, s-0.6) + 2\exp(x) s(1-s), \\ \dfrac{\partial X_2}{\partial s} - \nu_1 \dfrac{\partial^2 X_2}{\partial x^2} - \nu_2 (1+2x) \dfrac{\partial X_2}{\partial x} - 2\cos\left(\dfrac{\pi s}{4}\right) X_1 + 4\exp(1-s) X_2 = -2X_1(x, s-0.6) + (10x+1) s^2 (1-s)^2, \\ X_1(x,s) = 0, \;\; X_2(x,s) = 0, \;\; (x,s) \in \mathcal{M}_b, \\ X_1(0,s) = 0, \;\; X_1(1,s) = 0, \;\; X_2(0,s) = 0, \;\; X_2(1,s) = 0, \;\; s \in [0,1]. \end{cases}$$

Since the exact solutions to the above-described problems are unknown, we estimate the errors using the double mesh approach (see [1]). The error estimates for both components ($k = 1, 2$) are calculated as

$$\mathrm{E}_{k,\nu_1,\nu_2}^{\mathcal{N}_x,\mathcal{N}_s} = \max_{\substack{0 \le m \le \mathcal{N}_x \\ 0 \le n \le \mathcal{N}_s}} \left(|\widetilde{X}_k(x_{2m-1}, s_{2n-1}) - \widetilde{X}_k(x_m, s_n)| \right),$$

with the related convergence orders are given by

$$\mathrm{R}_{k,\nu_1,\nu_2}^{\mathcal{N}_x,\mathcal{N}_s} = \log_2 \left(\mathrm{E}_{k,\nu_1,\nu_2}^{\mathcal{N}_x,\mathcal{N}_s} / \mathrm{E}_{k,\nu_1,\nu_2}^{2\mathcal{N}_x,2\mathcal{N}_s} \right).$$

Additionally, we determine the ν_1 and ν_2 component-wise uniform maximum pointwise errors, by using $\mathrm{E}_{k,\nu_2}^{\mathcal{N}_x,\mathcal{N}_s}$ and $\mathrm{E}_{k,\nu_1}^{\mathcal{N}_x,\mathcal{N}_s}$ together with the corresponding ν_1 and ν_2-uniform orders of convergence $\mathrm{R}_{k,\nu_2}^{\mathcal{N}_x,\mathcal{N}_s}$ and $\mathrm{R}_{k,\nu_1}^{\mathcal{N}_x,\mathcal{N}_s}$ as follows

$$\mathrm{E}_{k,\nu_1}^{\mathcal{N}_x,\mathcal{N}_s} = \max_{\nu_2} \mathrm{E}_{k,\nu_1,\nu_2}^{\mathcal{N}_x,\mathcal{N}_s}, \quad \mathrm{E}_{k,\nu_2}^{\mathcal{N}_x,\mathcal{N}_s} = \max_{\nu_1} \mathrm{E}_{k,\nu_1,\nu_2}^{\mathcal{N}_x,\mathcal{N}_s},$$

$$\mathrm{R}_{k,\nu_1}^{\mathcal{N}_x,\mathcal{N}_s} = \frac{\log(\mathrm{E}_{k,\nu_1}^{\mathcal{N}_x,\mathcal{N}_s} / \mathrm{E}_{k,\nu_1}^{2\mathcal{N}_x,2\mathcal{N}_s})}{\log 2}, \quad \mathrm{R}_{k,\nu_2}^{\mathcal{N}_x,\mathcal{N}_s} = \frac{\log(\mathrm{E}_{k,\nu_2}^{\mathcal{N}_x,\mathcal{N}_s} / \mathrm{E}_{k,\nu_2}^{2\mathcal{N}_x,2\mathcal{N}_s})}{\log 2}.$$

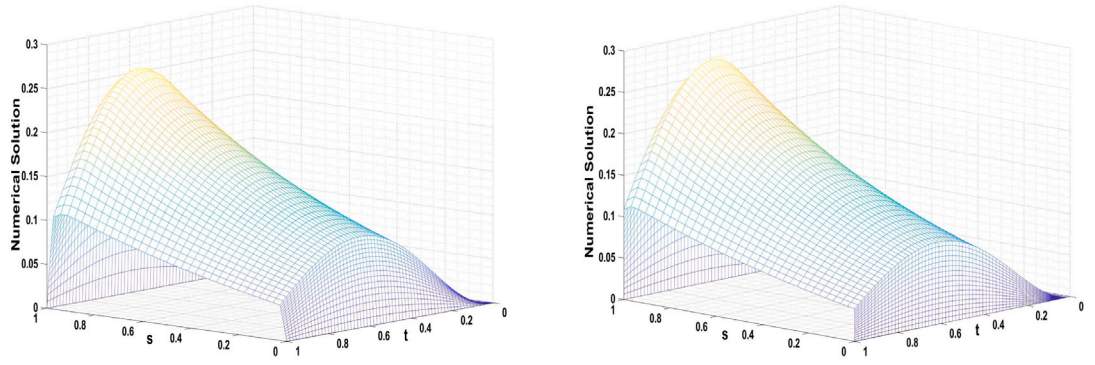

(a) $\nu_1 = 2^{-8},\ \nu_2 = 2^{-15}$ (b) $\nu_1 = 2^{-12},\ \nu_2 = 2^{-25}$

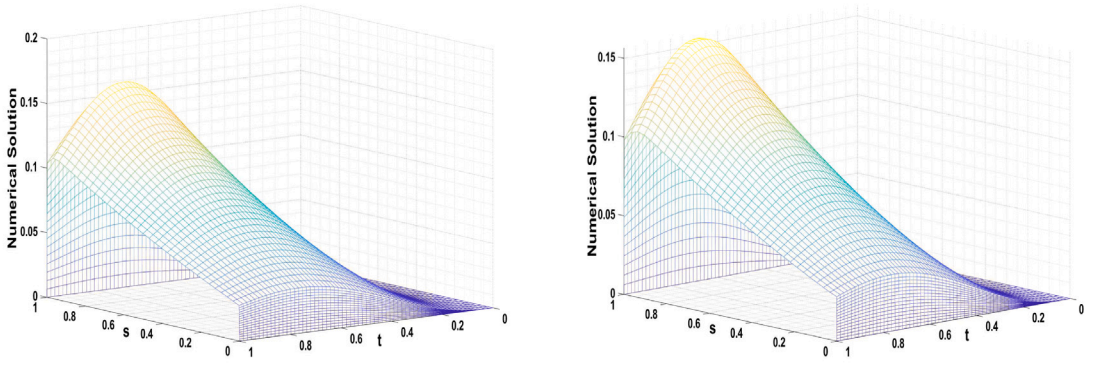

(c) $\nu_1 = 2^{-20},\ \nu_2 = 2^{-10}$ (d) $\nu_1 = 2^{-25},\ \nu_2 = 2^{-10}$

Fig. 4. Surface plots for Example 5.2's first and second solution components using various values of ν_1 and ν_2 with $\mathcal{N}_x = \mathcal{N}_s = 72$.

We begin by about the findings from the tabulated data. The error estimates for Example 5.1's first solution component are shown in Tables 2 and 4 for the case $\frac{\nu_2^2}{\nu_1} \ll 1$ and $\frac{\nu_2^2}{\nu_1} \gg 1$, respectively. Similarly, Tables 3 and 5 show these estimations for the second component of Example 5.1. Tables 7, 8, 9, and 10 show these findings for Example 5.2. The almost second-order parameter-uniform theoretically proved may be verified by looking at these tables. Table 6 displays the numerical errors alongside the estimated order of convergence to confirm the second-order accuracy in time; to see that, we multiplied N_x by 4 and N_s by 2. A value of order of convergence close to 2 confirms the second-order accuracy of the numerical scheme with respect to the time variable.

Each table also includes the CPU time (in seconds) taken for all values of the diffusion parameters at each column with N_x and N_s fixed, when we use the Block Thomas Algorithm to solve the linear systems related to the two test problems; from this table, we can observe that this CPU time is not very large and that it is not affected by the value of the convection and diffusion parameters.

Surface plots of solution components for various values of ν_1 and ν_2 for both cases are used to visually evaluate the boundary layers (see Figs. 1 and 4). At both extremities of the spatial domain, we see the presence of boundary layers. In order to show the existence of boundary layers, we also displayed the contour plots in Fig. 2((a) and (b)). The solution is plotted at different time levels in Fig. 2((c) and (d)). We find that the solution stays steady over time and exhibits the expected structure, proving the efficiency of the suggested approach. Furthermore, for smaller perturbation parameters, the presence of boundary layers is evident. The graphs corroborate the method's accuracy and robustness. To assess the accuracy of the numerical method, we plot the error graphs for different values of the perturbation parameter. From Fig. 3, we observe that the error decreases as the mesh is refined, confirming the convergence of the method.

6. Conclusions

This paper presents an effective numerical method for solving a two-parameter singularly perturbed system with a substantial time delay that consists of two coupled equations using spline basis functions. High accuracy and stability of the numerical solutions are ensured by the suggested technique, which successfully manages the difficulties presented by the existence of small perturbation parameters and considerable delay. An effective and reliable framework for capturing distinct boundary layers and resolving the

complex dynamics brought about by the delay term is provided by the combination of the Crank–Nicolson finite difference method for time discretization with the cubic spline collocation in space to discretize in space. The suggested method's accuracy and dependability are corroborated by the numerical results, which indicate that even for sufficiently small perturbation values, it generates reliable approximations. In order to improve the computing efficiency, future studies may concentrate on applying this paradigm to multidimensional problems and investigating adaptive mesh refining techniques.

CRediT authorship contribution statement

Parvin Kumari: Writing – original draft, Visualization, Validation, Software, Methodology, Investigation, Formal analysis, Conceptualization. **Carmelo Clavero:** Writing – review & editing, Visualization, Validation, Supervision, Methodology, Investigation, Formal analysis, Conceptualization.

Funding

The research of second author was partially supported by the project PID2022-136441NB-I00, the Aragón Government and the European Social Fund (group E24-17R).

Declaration of competing interest

The authors declare that they have no known competing financial interests or personal relationships that could have appeared to influence the work reported in this paper.

Acknowledgments

The authors gratefully acknowledge the valuable comments and suggestions from the anonymous referees to improve this work.

References

[1] C. Clavero, J.L. Gracia, J.C. Jorge, High-order numerical methods for one-dimensional parabolic singularly perturbed problems with regular layers, Numer. Meth. Part. Diff. Equ. 21 (2005) 149–169.
[2] R.E. O'Malley, Introduction To Singular Perturbations, Academic Press, 2014.
[3] M. Ghil, A.W. Robertson, Climate dynamics and predictability, Bull. Amer. Meteo. Soc. 83 (2002) 571–591.
[4] E.l. Mehdi Lotfi, Y. Radouane, Y. Noura, A generalized reaction–diffusion epidemic model with time delay, Discon. Nonli. Compl. 3 (1) (2014) 1–6.
[5] J.D. Murray, Mathematical Biology I: An Introduction, Springer, 2002.
[6] M. Amrein, T.P. Wihler, Fully adaptive Newton-Galerkin time stepping methods for singularly perturbed parabolic evolution equations, 2015, https://arxiv.org/abs/1510.00622.
[7] S. Cengizci, N. Srinivasan, M.T. Atay, A hybrid simulation for a system of singularly perturbed two-point reaction–diffusion equations, 2017, arXiv preprint arXiv:1710.01694.
[8] D. Kumar, P. Kumari, Fitted mesh B-spline collocation method for singularly perturbed differential–difference equations with small delay, J. Comput. Appl. Math. 339 (2018) 1–15.
[9] D. Kumar, P. Kumari, A parameter-uniform scheme for singularly perturbed partial differential equations with a time lag, Numer. Meth. Part. Diff. Equ. 36 (2020) 1–20.
[10] M.A. Woldaregay, Novel numerical scheme for singularly perturbed time delay convection-diffusion equation, Adv. Math. Phys. 2021 (2021) 6641236.
[11] S. Kumar, M. Kumar, An efficient hybrid numerical method based on an additive scheme for solving coupled systems of singularly perturbed linear parabolic problems, Math. Methods Appl. Sci. 46 (2023) 1234–1256.
[12] I.T. Daba, W.G. Melesse, G.D. Kebede, An efficient numerical approach for singularly perturbed time delayed parabolic problems with two-parameters, BMC Res. Notes 17 (1) (2024).
[13] P. Kumari, S. Singh, D. Kumar, An effective numerical approach for solving a system of singularly perturbed differential–difference equations in biology and physiology, Math. Comput. Simulation 229, 553–573.
[14] C. Clavero, S. Kumar, S. Kumar, A priori and a posteriori error estimates for efficient numerical schemes for coupled systems of linear and nonlinear singularly perturbed initial-value problems, Appl. Num. Meth. 208 (2025) 123–147.
[15] C. Clavero, R. Shiromani, V. Shanthi, A numerical approach for a two-parameter singularly perturbed weakly-coupled system of 2-D elliptic convection-reaction–diffusion PDE, J. Comput. Appl. Math. 436 (2024) 115422, http://dx.doi.org/10.1016/j.cam.2023.115422.
[16] C. Clavero, R. Shiromani, V. Shanthi, A computational approach for 2D elliptic singularly perturbed weakly-coupled systems of convection–diffusion type with multiple scales and parameters in the diffusion and the convection terms, Math. Methods Appl. Sci. 47 (2024) 13510–13541, http://dx.doi.org/10.1002/mma.10204.
[17] C. Clavero, R. Shiromani, An efficient numerical method for 2D elliptic singularly perturbed systems with different magnitude parameters in the diffusion and the convection terms, part II, AIMS Math. 9 (12) (2024) 35570–35598, DOI:10.934/math.20241688.
[18] C. Clavero, R. Shiromani, An efficient numerical method for 2D elliptic singularly perturbed systems with different magnitude parameters in the diffusion and the convection term, Comput. Math. Appl. 181 (2025) 287–322, http://dx.doi.org/10.1016/j.camwa.2025.01.011.
[19] O.A. Ladyženskaja, V.A. Solonnikov, N.N. Ural'tseva, Linear and Quasilinear Equations of Parabolic Type, Translated from the Russian By S. Smith, in: Transl. Math. Monog., vol. 23, Amer. Math. Soc., Providence, 1968.
[20] Mishra, H. Kumar, S. Saini, Various numerical methods for singularly perturbed boundary value problems, Ame. J. Appl. Math. Stat. 2 (2014) 129–142.
[21] D. Avijit, S. Natesan, SDFEM for singularly perturbed boundary-value problems with two parameters, J. Appl. Math. Comput. 64 (2020) 591–614.
[22] N. Kumari, S. Gowrisankar, A robust B-spline method for two parameter singularly perturbed parabolic differential equations with discontinuous initial condition, J. Appl. Math. Comput. 70 (2024) 5379–5403.
[23] E. O'Riordan, M.L. Pickett, G.I. Shishkin, Parameter-uniform finite difference schemes for singularly perturbed parabolic diffusion-convection-reaction problems, Math. Comp. 75 (2006) 1135–1154.

[24] S. Singh, P. Kumari, D. Kumar, An effective numerical approach for two parameter time-delayed singularly perturbed problems, Comput. Appl. Math. 41 (2022) http://dx.doi.org/10.1007/s40314-022-02046-3.
[25] T. Linß, H.G. Roos, Analysis of a finite-difference scheme for a singularly perturbed problem with two small parameters, J. Math. Anal. Appl. 289 (2004) 355–366.
[26] D. Kumar, A uniformly convergent scheme for two-parameter problems having layer behaviour, Int. J. Comp. Math. 99 (3) (2021) 553–574.
[27] S. Singh, D. Kumar, Parameter uniform numerical method for a system of singularly perturbed parabolic convection–diffusion equations, Math. Comput. Simulation 212 (2023) 360–381.
[28] C.A. Hall, On error bounds for spline interpolation, J. Approx. Theo. 1 (1968) 209–218.
[29] J.M. Varah, A lower bound for the smallest singular value of a matrix, Linear Algebra Appl. 11 (1975) 3–5.